# Functions and mechanics of dynein motor proteins

Anthony J. Roberts[1,2], Takahide Kon[3,4], Peter J. Knight[1], Kazuo Sutoh[5] and Stan A. Burgess[1]

Abstract | Fuelled by ATP hydrolysis, dyneins generate force and movement on microtubules in a wealth of biological processes, including ciliary beating, cell division and intracellular transport. The large mass and complexity of dynein motors have made elucidating their mechanisms a sizable task. Yet, through a combination of approaches, including X-ray crystallography, cryo-electron microscopy, single-molecule assays and biochemical experiments, important progress has been made towards understanding how these giant motor proteins work. From these studies, a model for the mechanochemical cycle of dynein is emerging, in which nucleotide-driven flexing motions within the AAA+ ring of dynein alter the affinity of its microtubule-binding stalk and reshape its mechanical element to generate movement.

[1]Astbury Centre for Structural Molecular Biology, School of Molecular and Cellular Biology, Faculty of Biological Sciences, University of Leeds, Leeds LS2 9JT, UK.
[2]Department of Cell Biology, Harvard Medical School, 240 Longwood Avenue, Boston, Massachusetts 02115, USA.
[3]Department of Frontier Bioscience, Faculty of Bioscience and Applied Chemistry, Hosei University, 3-7-2 Kajino-cho, Koganei, Tokyo 184-8584, Japan.
[4]Japan Science and Technology Agency, PRESTO, 4-1-8 Honcho, Kawaguchi, Saitama 332-0012, Japan.
[5]Faculty of Science and Engineering, Waseda University, Okubo 3-4-1, Shinjuku-ku, Tokyo 169-8555, Japan.
Correspondence to A.J.R and S.A.B
e-mails: Anthony_Roberts@hms.harvard.edu; S.A.Burgess@leeds.ac.uk

To move, divide and spatially organize their teeming interiors, eukaryotic cells use ATP-fuelled motor proteins to generate forces and transport cargoes along cytoskeletal tracks. The numerous proteins, organelles and mRNAs that undergo directed transport by motor proteins touch on a wide range of cellular and developmental processes. Underscoring the importance of cytoskeletal motors in biology, it is now clear that serious human and animal diseases arise from motor protein dysfunction[1,2].

Dynein is one of the three families of cytoskeletal motor protein. Originally identified 50 years ago as an ATPase in *Tetrahymena pyriformis* cilia[3], dynein was named by Gibbons and Rowe after the unit of force, the dyne[4]. A cytoplasmic form of dynein was subsequently isolated from brain tissue[5] and shown to drive intracellular transport towards the minus ends of microtubules[6,7], which typically lie in the microtubule-organizing centre near the nucleus in non-dividing cells (FIG. 1). The discovery of dynein thus complemented the finding of kinesins[8]; microtubule-based motors that typically move towards the plus ends of microtubules and hence the cell periphery.

Given that dyneins and kinesins both move along microtubules, one might have expected their mechanisms of motility to have more in common with one another than with the actin-based motor, myosin. It was therefore a surprise when crystal structures of myosin and kinesin revealed that — despite moving on different cytoskeletal polymers — these motors share a G protein-related fold and similarities in their core mechanisms[9].

Dynein is currently at the frontier of cell motility research at the molecular level, as its mechanism of movement is much less well understood than that of kinesin and myosin. Dubbed the 'big wheel' of motor proteins[10], dynein belongs to the AAA+ superfamily (ATPases associated with diverse activities)[11]. Conventional AAA+ ATPases function as hexameric rings that unfold proteins, dismantle DNA and RNA duplexes and pry apart macromolecular complexes and aggregates[11]. Like conventional AAA+ ATPases, dynein has a ring of six AAA+ modules at its core but, unusually, these are linked together into one large polypeptide, along with several unique appendages that enable motor function. The large size and complexity of dynein have made elucidating its mechanism a formidable task. However, recent studies have risen to this challenge using various approaches. For example, in the past 2 years, long sought-after crystal structures of the motor domain of dynein have been solved, and single-molecule studies, live-cell imaging and electron microscopy have provided key insights into the dynamics of dynein.

In this Review, we focus on advances in two main areas: first, the cellular functions of dyneins, and second, the molecular mechanism of the dynein motor domain. Exciting progress has also been made in understanding how dyneins are regulated and recruited to specific cargoes in the cell, and the reader is referred to recent reviews on these topics[12–19].
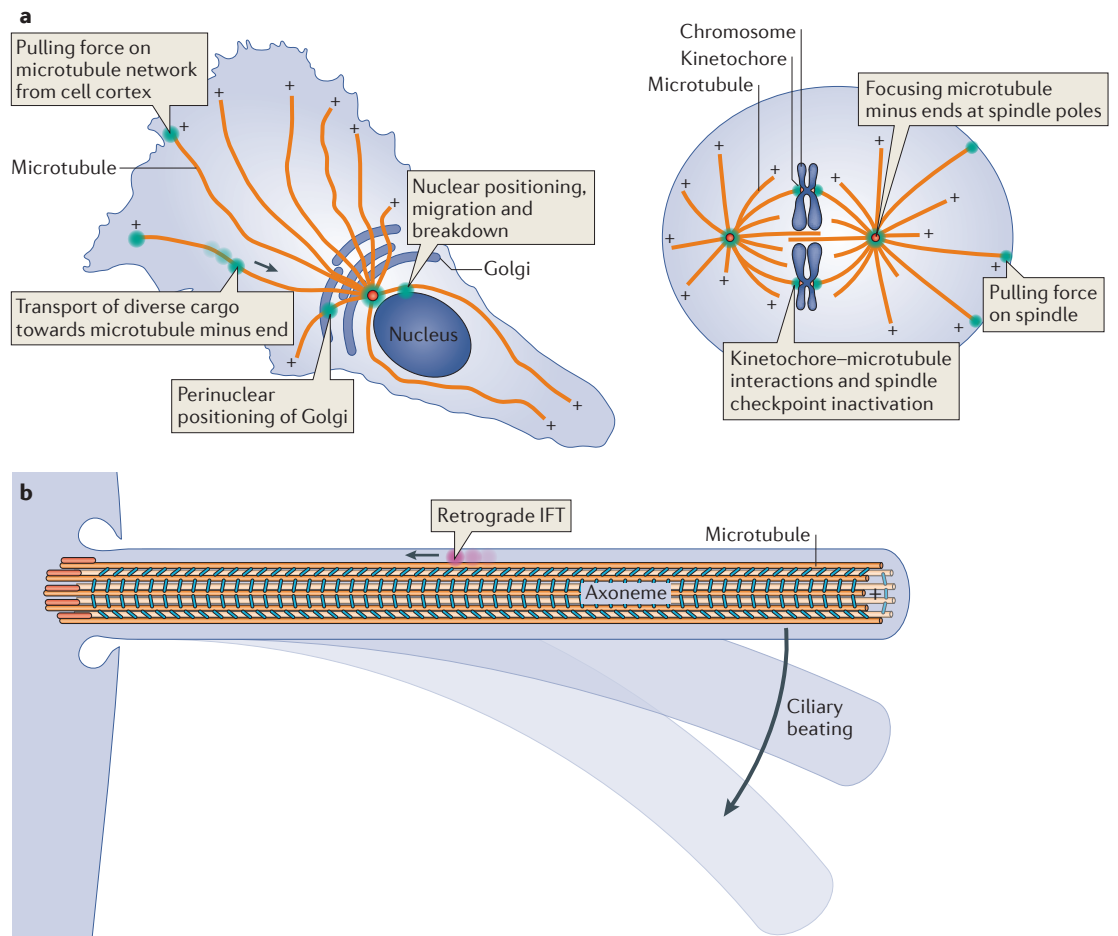
Figure 1 | **Sites of dynein action in the cell.** **a** | Example functions of cytoplasmic dynein (green) are shown in an interphase cell (left) and a dividing cell (right). The polarity of microtubules is indicated by plus signs. The arrow depicts the direction of dynein movement towards the microtubule minus end. Note that in some cell types and regions, such as the dendritic arbors of neurons, the microtubule network can have mixed polarity. **b** | Dynein functions in cilia. Intraflagellar transport (IFT) dynein (pink) performs retrograde IFT, whereas axonemal dyneins (cyan) power the beating of motile cilia.

## Overview of the dynein family

Dyneins operate as protein complexes built around force-generating subunits called heavy chains, so termed because of their large molecular mass (typically ~500 kDa) (FIG. 2). Each heavy chain contains a motor domain that belongs to the AAA+ superfamily[11] attached to a divergent amino-terminal tail domain (FIG. 2a). The tail specifies distinct oligomerization properties and serves as a platform for the binding of several types of associated subunit (FIG. 2b), which in turn mediate interactions with cargo either via direct binding or through the recruitment of adaptor proteins.

Phylogenetically, there are nine major classes of dynein heavy chain[20]. The cytoplasmic dynein 1 heavy chain (encoded by *DYNC1H1* in humans) is used for nearly all of the minus end-directed transport in the cytoplasm of most eukaryotic cells (FIG. 1a). However, archaeplastidans, which lack dyneins and possess an expanded repertoire of minus end-directed kinesins[21], are an exception. Cytoplasmic dynein 2 (encoded by *DYNC2H1* in humans) has a specialized role in transporting material along motile and sensory cilia and flagella (FIG. 1b).

In this Review, we refer to cytoplasmic dynein 1 as 'cytoplasmic dynein' and cytoplasmic dynein 2 as 'intraflagellar transport (IFT) dynein' for distinction. The remaining seven dynein classes are built into the axoneme, where they power ciliary beating (BOX 1). Some axonemal dynein classes have multiple representatives per genome, so the total number of distinct heavy chain genes in organisms that build a motile axoneme typically exceeds nine. For example, there are 16 dynein heavy chain genes in the human genome[22].

## Functions of cytoplasmic dynein

Cytoplasmic dynein performs a great variety of cellular functions. The breadth of these activities seems to be greatest in metazoan cells (described below), but cytoplasmic dynein is also used to varying extents in fungi, alveolata, stramenopila and amoebozoa[20]. For example, in the yeast *Saccharomyces cerevisiae*, the sole known role of cytoplasmic dynein is positioning the nucleus during cell division[23], whereas in filamentous fungi[24] and the slime mould *Dictyostelium discoideum*[25] it is also used for vesicle transport.

---

**G protein-related fold**
A characteristic arrangement of secondary structure elements and loops (such as switch I and switch II) shared by G proteins, myosins and kinesins, which indicates that these proteins originated from a common ancestor.

**Axoneme**
The microtubule-based core of eukaryotic cilia and flagella. The terms cilia and flagella are often used interchangeably, as both describe cellular appendages with an axoneme at their core. In this Review, we use cilia for consistency.
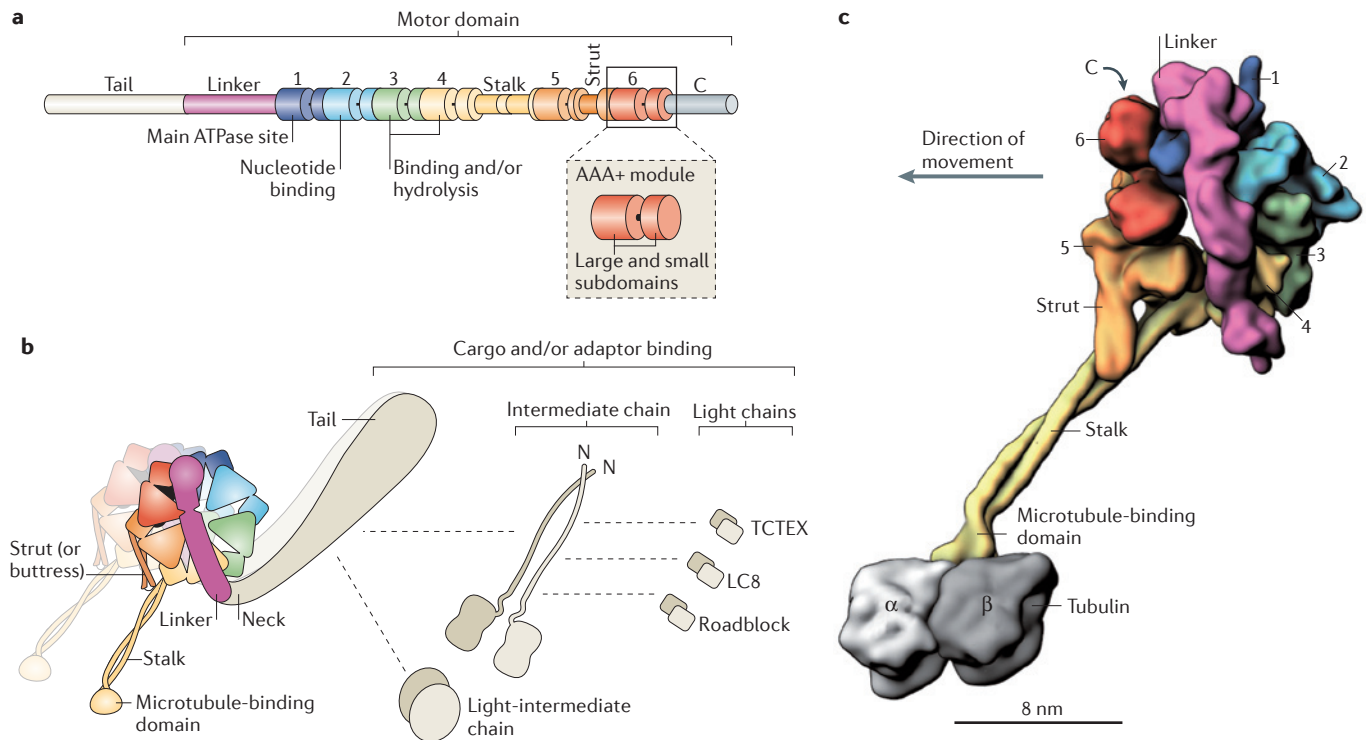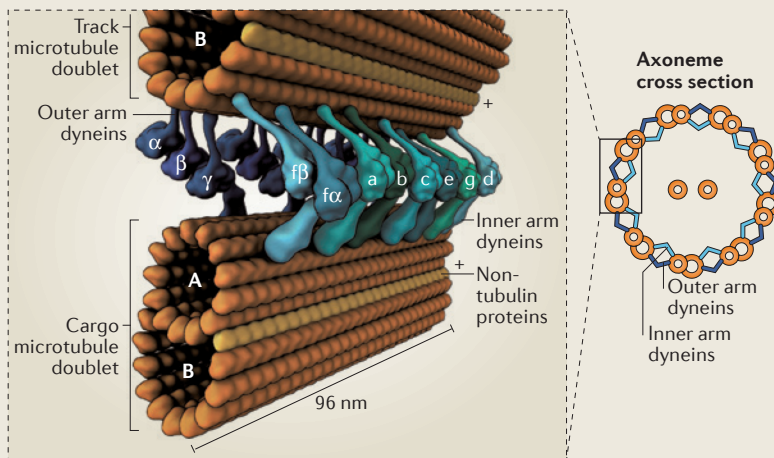
Figure 2 | **Overview of dynein composition. a** | Linear representation of domains within the dynein heavy chain. The amino-terminal tail domain is involved in dynein oligomerization, cargo-binding and regulation, but is not part of the minimal motor domain capable of producing movement *in vitro*. The motor domain comprises the linker domain, six AAA+ modules (1–6), the coiled-coil stalk and strut, and the carboxy-terminal region. The motor domain of *Dictyostelium discoideum* dynein has a molecular mass of ~380 kDa. In many fungal dyneins, the C-terminal region is shorter and the motor domain is ~330 kDa. Each of the AAA+ modules is composed of a large N-terminal subdomain and a smaller C-terminal subdomain (see inset and BOX 2). **b** | The cytoplasmic dynein complex contains a pair of identical heavy chains. Within each heavy chain, the six AAA+ modules fold into a ring. The stalk protrudes as an extension from the small subdomain of AAA4. The tail is connected to AAA1 by the linker domain, which arches over the AAA+ ring. In *Chlamydomonas reinhardtii* inner arm dynein-c, a sharp ~90° kink exists between the linker and the tail[90,92,115]. Although not yet visualized in cytoplasmic dynein, a similar kink might exist, as it would prevent a steric clash between the tail and the microtubule. In dynein-c, this neck region of the tail is a natural site of flexibility in the molecule, allowing the angle of the tail to vary with respect to the motor domain[90,92,115]. The cytoplasmic dynein heavy chains assemble with up to five types of associated subunit, which are also dimers[148]. The associated subunits comprise the intermediate chain, the light-intermediate chain and three classes of light chain: TCTEX, LC8 and Roadblock. Dashed lines indicate reported interactions of the associated subunits with each other and with the tail[26]. The three-dimensional (3D) arrangement of the associated subunits with respect to the tail is unknown. **c** | A 3D model of the cytoplasmic dynein motor domain bound to the microtubule (the associated subunits are not shown). As no high-resolution structure currently exists for the entire motor domain bound to a tubulin dimer, this model is based on a 2.8 Å crystal structure of the *D. discoideum* dynein motor domain lacking the microtubule-binding domain[93] (Protein Data Bank ID: 3VKG), joined to a cryo-electron microscopy-derived model of the mouse microtubule-binding domain bound to an α-tubulin–β-tubulin dimer[112] (Protein Data Bank ID: 3J1T). Subdomains are shown in surface representation, with the two long α-helices in the stalk rendered separately to emphasize their coiled-coil arrangement. The six AAA+ modules are numerically labelled.

Cytoplasmic dynein assembles around two identical heavy chains and is thus known as a two-headed motor. A pressing question is how this assembly can be directed to its many sites of action in the cell (FIG. 1a). At least part of the answer lies in the large complement of additional subunits in the complex (FIG. 2b). Metazoan genomes encode five classes of associated subunit, each of which functions as a dimer; these are the intermediate chain, light-intermediate chain and three types of light chain (TCTEX, LC8 and Roadblock). Moreover, in mammals, there are two genes for each class of subunit, some of which have restricted expression patterns in the body[26]. Diversity in the associated subunits is compounded by

differentially spliced and phosphorylated isoforms[26]. Recent reconstitution of the human cytoplasmic dynein complex has revealed that the associated subunits can serve critical structural roles, as the heavy chain forms aggregates instead of dimers in the absence of the light-intermediate chain[27].

In addition to these core components of the complex, cytoplasmic dynein interacts with three ubiquitous regulators: lissencephaly 1 (LIS1; also known as NUDF), nuclear distribution E (NUDE) and the dynactin complex. These important regulators alter the intrinsic mechanical behaviour of cytoplasmic dynein and are involved in most, if not all, of its cellular functions. Therefore, a

## Box 1 | Functions of dynein in the axoneme



Observed in cross-section, the axoneme has a characteristic '9 + 2' appearance in many eukaryotes, corresponding to nine peripheral doublet microtubules surrounding a central pair of singlet microtubules (see the figure). Each doublet consists of a complete microtubule with 13 protofilaments (termed the A-tubule) and an incomplete microtubule of 10 protofilaments (termed the B-tubule), with non-tubulin proteins at the junction[138]. Microtubule polarity is indicated by plus signs. Numerous additional proteins, such as radial spokes, nexin–dynein regulatory complexes and microtubule inner proteins (not shown), have crucial roles in axoneme motility, structure and regulation.

Within motile axonemes, dyneins drive the sliding of adjacent microtubule doublets relative to each other[139]. These sliding motions are resisted by other axonemal components, converting them into bending deformations that propagate along the axoneme. The resulting oscillations can either propel the cell through its fluid environment or create flow over the cell surface. To produce sliding, axonemal dyneins form a stable attachment to a cargo microtubule via their tails and use their motor domains to translocate along an adjacent track microtubule.

Axonemal dyneins subdivide into inner and outer arms, depending on their position[3]. Their arrangement is currently best characterized in the green algae *Chlamydomonas reinhardtii*, in which detailed insights have come from molecular genetic and cryo-electron tomography studies[140]. Each outer arm consists of three different dynein heavy chains (α-, β- and γ-chain; see the figure), which adopt a stacked arrangement and co-purify as a complex with ~15 smaller subunits[141]. The outer arms repeat at 24 nm intervals along the axoneme and are crucial for generating the proper beat frequency. The inner arms comprise eight different dynein heavy chains (one heterodimer (fα and fβ) and six monomers (a–e and g), each with its own complement of associated subunits), which repeat with a 96-nm periodicity[142]. Each inner arm dynein has distinct motile properties and roles in shaping the ciliary waveform[143].

From this general layout, dynein composition can vary both around and along the axoneme. For example, in *C. reinhardtii*, three specialized heavy chains replace canonical inner arm dyneins near the base of the axoneme[144], and one of the doublets lacks outer arms along its length[142]. In most metazoans, each outer arm contains two heavy chains, rather than three. The 9 + 2 arrangement also varies in some organisms. For instance, the highly motile sperm axoneme of the eel *Anguilla anguilla* is a minimal 9 + 0 structure that lacks outer arms, radial spokes and the central pair of microtubules[145]. These structural variations probably contribute to the distinct waveforms and motile properties displayed by cilia. In all systems, for wave-like bending motions to occur, zones of dynein activity are proposed to switch from one side of the axoneme to the other, and to propagate along its length. Models for the coordination and regulation of dynein activity are discussed in REFS 16–19. How axonemal dyneins assemble into this configuration and work as an integrated system, with the many regulators and structural proteins in the axoneme, is only beginning to emerge.

complete understanding of cytoplasmic dynein motility requires a detailed dissection of how dynactin, NUDE and LIS1 act on dynein, and progress towards this goal has been reviewed recently[12–14,28].

*Cargo transport along cytoplasmic microtubules.* Cytoplasmic dynein powers the transport of membrane-bound vesicles and tubules, together with their resident molecules, towards microtubule minus ends (FIG. 1a). Examples of organelles trafficked by cytoplasmic dynein include endosomes[29], lysosomes[30], phagosomes[31], melanosomes[32], peroxisomes[33], lipid droplets[34], mitochondria[35] and vesicles from the endoplasmic reticulum (ER) destined for the Golgi[36]. Such transport can transmit signals between different parts of the cell. For example, at nerve terminals, stimulated tropomyosin-receptor kinase (TRK) receptors are internalized into endosomes and transported by dynein towards the cell body, where they initiate signalling cascades essential for neuron survival[37]. Additional types of cytoplasmic dynein cargo include components of the centrosome[38], transcription factors[39], cytoskeletal filaments[40] and mRNA-containing ribonucleoprotein complexes[41]. Cytoplasmic dynein is also involved in clearing material from the periphery of the cell for degradation and recycling[42,43]: at the distal tip of neurons, organelles and proteins are engulfed into autophagosomes and transported in a dynein-dependent manner towards the cell body for breakdown[43]. Furthermore, viruses such as HIV, herpesvirus and adenovirus have evolved mechanisms to hijack cytoplasmic dynein to reach the nucleus[44]. Finally, although cytoplasmic dynein typically moves its cargo through the intracellular space, recent studies raise the idea that it can also translocate membrane-spanning proteins and signalling complexes in the plane of the lipid bilayer, for instance within the nuclear envelope[45,46] and at the immunological synapse[47,48].

*Exerting tension on cellular structures.* Cytoplasmic dynein executes additional functions by associating with cellular structures and exerting tension on microtubules. For example, dyneins tethered at the cell cortex can apply a pulling force on the microtubule network (FIG. 1a) by either walking towards the minus end of a microtubule or coupling to a disassembling plus end[49,50]. In doing so, cytoplasmic dynein is thought to pull the microtubule cytoskeleton towards the leading edge of migrating neurons[51] and fibroblasts[52] or towards the immunological synapse in T cells[53].

The pulling force of dynein is also used during cell division[54]. By hauling on astral microtubules that emanate from the spindle, cytoplasmic dynein can cause the spindle to oscillate or to localize towards one end of the cell. Remarkably, during spindle oscillation in mammalian cells, cortical dynein dynamically redistributes from one side of the cell to the other, dissociating from its cortical receptors when the spindle pole is within ~2 μm and accumulating with them when the spindle pole moves further away[55,56].

In large cells, such as amphibian embryos, dynein seems to exert pulling forces on microtubule asters even when the microtubules are not long enough to reach the cell cortex[57]. Recent studies indicate that this can occur as the dynein-driven movement of organelles along microtubules generates sufficient viscous drag to slowly pull the microtubule network in the opposite direction[57–59].

An appealing feature of this model is that the pulling force would vary according to microtubule length (as net organelle transport will be greater on longer microtubules). In embryos, length-dependent pulling is proposed to be a key ingredient for aster centring and spacing[57,58].

Further cellular structures that are connected to the microtubule network by cytoplasmic dynein are the Golgi and the nuclear envelope. Indeed, the perinuclear positioning of the Golgi during interphase depends on cytoplasmic dynein[60] (FIG. 1a). At the outer nuclear envelope, dynein has been reported to contribute to nuclear rotation[61] and positioning[51], centrosome separation[62] and the breakdown of the nuclear envelope for open mitosis[63].

*Functions at the spindle and kinetochore.* At cell division, cytoplasmic dynein assists in assembling microtubules into the chromosome-segregating device known as the spindle (FIG. 1a). Specifically, studies using frog egg extracts reveal that dynein is required to focus the minus ends of microtubules at the spindle poles[64,65]. The mechanism remains to be elucidated, but a leading model is that dynein slides antiparallel microtubules apart so that their plus ends project outward and their minus ends are gathered. The dynein-powered transportation of other spindle components, such as nuclear mitotic apparatus (NUMA), also plays a part in the construction of this large microtubule-based structure[65].

Finally, cytoplasmic dynein localizes to the kinetochore — the protein assembly that links centromeric DNA to spindle microtubules. Kinetochore dynein has an important role in the molecular surveillance mechanism that aids faithful chromosome segregation by delaying anaphase until all chromosomes are properly attached to the spindle[66]. When the plus ends of spindle microtubules have stably engaged with the kinetochores, cytoplasmic dynein is thought to remove spindle-assembly checkpoint proteins by transporting them towards the spindle poles[67,68]. In mammalian cells, cytoplasmic dynein is also reported to help maintain initial spindle–kinetochore attachments and drive rapid poleward chromosome movements during their alignment at the metaphase plate[69,70].

### IFT dynein

IFT dynein, which is closely related to cytoplasmic dynein, also functions as a cargo transporter but operates within the confines of the cilium (FIG. 1b). Although motile and sensory cilia form stable steady-state structures, their building blocks are continually turning over[71]. Through the process of IFT, new components are trafficked towards the tip of the cilium, material is moved back to the base, and signalling receptors are distributed in the plane of the membrane. IFT dynein transports cargo towards the base of the cilium[72,73], where the microtubule minus ends reside. Members of the kinesin 2 family drive cargo transport to the tip. IFT dynein functions as a homodimer of heavy chains and associated subunits, although relatively little is known about its motile properties[74–76]. Observations in *Chlamydomonas reinhardtii* indicate that minus end-directed IFT involves the movement of oligomeric particles (also termed 'trains') of material ~250 nm

long, which form multiple contacts with the outer surface of the axoneme[77]. Moreover, the forces generated by retrograde IFT trains exceed those of a single motor[78,79], indicating that IFT dynein works in multi-motor collectives *in situ*. This property is akin to the mode of action of cytoplasmic dynein, which also carries out many of its tasks in teams of motors (reviewed in REF. 80).

### Dynein motor structure and mechanism

At the core of all dynein functions is the action of the motor domain. This carboxy-terminal region of the heavy chain (FIG. 2a) can be recombinantly expressed as a stable monomeric entity[81] and contains all of the elements that are needed to convert the energy from ATP hydrolysis into movement[27,82–84]. Evidence suggests that this process occurs through a mechanochemical cycle, in which chemical transitions (ATP binding, ATP hydrolysis and the release of inorganic phosphate ($P_i$) and ADP) are coupled to structural changes in the motor and, conversely, mechanical events (such as microtubule binding) can influence the rate of chemical transitions. Although certain parameters such as the overall cycle rate vary among dynein classes, probably reflecting their specialization to particular cellular functions, current data suggest that cytoplasmic and axonemal dynein use a conserved basic mechanism.

*Mechanochemical cycle.* In an overview of the dynein operating cycle, ATP induces dissociation of the motor–microtubule complex[85]. After detaching from the microtubule, the motor rearranges, becoming primed for a subsequent structural change (termed the powerstroke) that is thought to generate force. Next, following a diffusive search, rebinding of the motor to a new site on the microtubule stimulates the release of ATP hydrolysis products, thus triggering the powerstroke[86] (FIG. 3).

At first glance, the chemical and mechanical events in the dynein cycle bear a strong resemblance to those of the actin-based motor myosin 2. This striking piece of convergent evolution became clear from early studies of outer arm axonemal dyneins[87]. However, a look 'under the hood' of the motor domain of dynein reveals that its ancestry in the AAA+ superfamily makes its mechanism of action quite distinct from the other cytoskeletal motor classes.

*Motor domain architecture.* FIGURE 2c depicts the architecture of the dynein motor domain, which has been uncovered through sequence analysis, two-dimensional (2D) electron microscopy and, most recently, X-ray crystallography and three-dimensional (3D) cryo-electron microscopy (cryo-EM)[11,88–96]. The N-terminal part of the motor forms an elongated linker domain that arches over the catalytic region and is thought to deliver the powerstroke. The catalytic core of dynein contains six AAA+ modules, which fold into a ring akin to that of other AAA+ machines. However, unlike canonical AAA+ hexamers, which are oligomeric, the six AAA+ modules of dynein are joined together in the same polypeptide by short connecting sequences and have different properties (FIG. 2a). For example, only the first four

**Autophagosomes**
Organelles that enwrap cytoplasmic material in a double-membrane-bound structure and subsequently fuse with lysosomes, leading to degradation of the confined material.

**Immunological synapse**
The interface formed between an antigen-presenting cell and a lymphocyte, such as a B cell or a T cell.

**Astral microtubules**
Microtubules radiating from the spindle poles that do not contact the kinetochore or overlap with other microtubules in the spindle midzone.
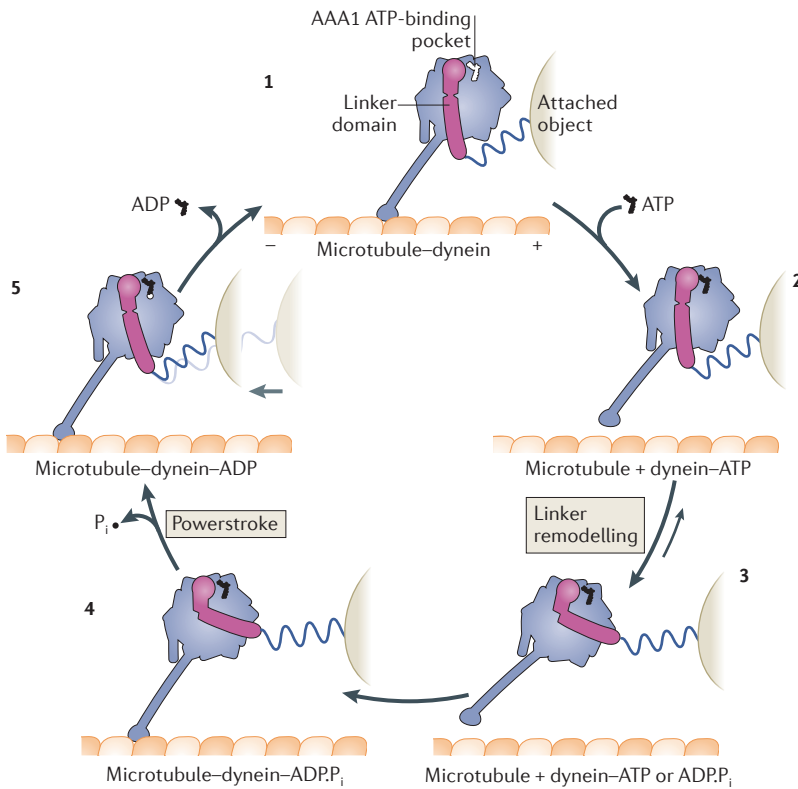
Figure 3 | **Model of the mechanochemical cycle of a cytoplasmic dynein motor domain.** Model for the *Dictyostelium discoideum* cytoplasmic dynein motor domain[85,86,91,93,111,118]. Plus and minus signs indicate microtubule polarity. The dynein motor domain moves towards the minus end of the microtubule. Force exerted on an attached object is shown schematically by the stretching of a spring, which does not represent a part of the dynein structure. Conceptually, the attached object could represent a partnering motor domain in a cytoplasmic dynein dimer or the cargo microtubule of an axonemal dynein. With no nucleotide bound at the AAA1 ATPase site, the dynein motor domain is tightly bound to the microtubule (1). ATP binding induces rapid dissociation from the microtubule (2) (FIG. 4). The dissociation rate is ~460 s$^{-1}$ for the *D. discoideum* dynein motor domain[85]. A slower ATP-driven change (~200 s$^{-1}$) is the remodelling of the linker domain[85], which is displaced across the AAA+ ring (3) (FIG. 5). Remodelling of the linker extends the search range of the microtubule-binding domain along the microtubule. After hydrolysis of ATP to ADP and inorganic phosphate (P$_i$), the motor domain is thought to engage a new binding site on the microtubule, initially via a weak interaction (4). Strong binding to the microtubule accelerates the release of P$_i$ from AAA1, inducing the linker to revert to its straight form. This transition is speculated to represent the powerstroke: the main step in which force (indicated by the light grey arrow) is transmitted to the attached object (5). Finally, ADP is released from AAA1 and the cycle restarts. The occupancy of other nucleotide-binding AAA+ modules of dynein, AAA2, AAA3 and AAA4, during the cycle, is unknown. Although the cycle is shown starting with dynein having no nucleotide bound at AAA1, it is not meant to imply that this is the longest-lived state. Indeed, *in vivo*, where the ATP concentration is in the millimolar range, ATP would rapidly bind at AAA1 once ADP is released, and thus this state would be populated only transiently.

**Crystal soaking**
A technique in which a crystallized macromolecule is bathed in a ligand-containing solution. The ligand has the opportunity to bind the macromolecule of interest owing to diffusion through solvent-filled channels in the crystal.

modules (AAA1–AAA4) contain functional nucleotide-binding motifs. On the face opposite the linker, the ring is embellished with a C-terminal domain that interacts mainly with AAA5 and AAA6. The microtubule-binding domain lies at the tip of a ~15 nm antiparallel coiled-coil stalk that protrudes as a pair of α-helices from AAA4. Near its base, the stalk interacts with a second coiled-coil strut (also known as the buttress) that emerges from AAA5. This expansive architecture, which places the sites of ATP breakdown and microtubule binding ~25 nm apart, makes long-range structural changes a central part of the dynein mechanism.
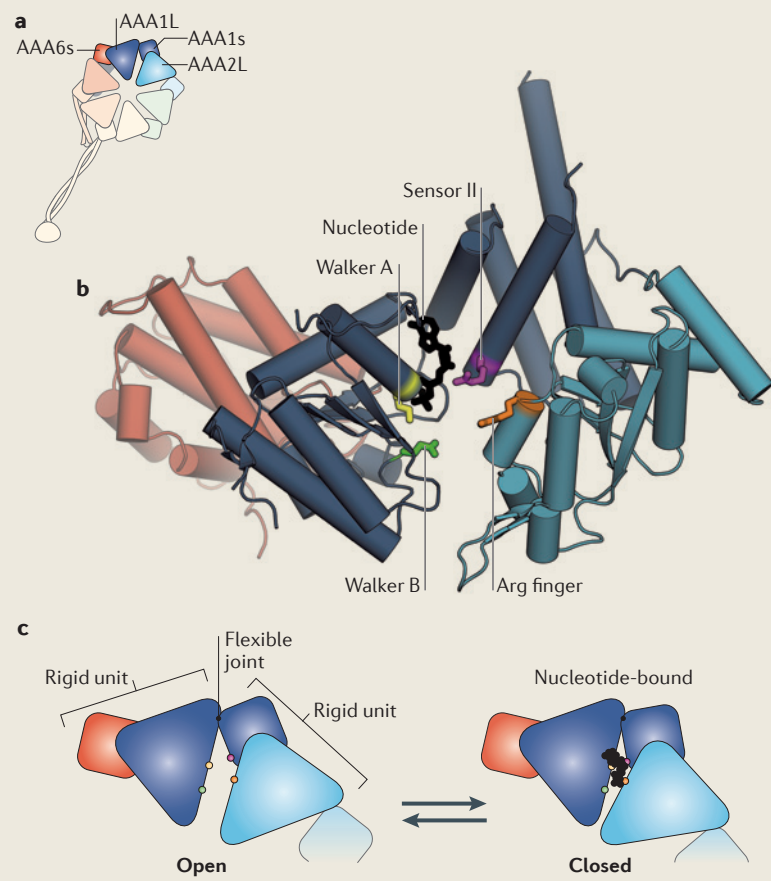
*The AAA+ ring.* The AAA+ ring can be thought of as the engine of dynein as it converts the chemical energy from ATP hydrolysis into motion. Each AAA+ module consists of a large and a small subdomain, which are connected by a flexible joint[93–96] (BOX 2). To form a ring, the small subdomain of one AAA+ module packs against the large subdomain of the neighbouring module. This layout produces six tight interfaces (between the AAA+ modules) and six potential hinges (one within each AAA+ module), as seen in prior structures of AAA+ hexamers[97,98]. Based on these earlier studies, nucleotide transactions in the AAA+ modules are expected to alter the angles of the hinges and cause flexing of the ring.

*Opening and closing of AAA1.* Mutagenesis and biochemical experiments suggest that AAA1 is the main site of ATP hydrolysis in the dynein ring[99,100]. Accordingly, it displays the hallmarks of an AAA+ nucleotide-binding pocket, as seen in a 2.8 Å structure of *D. discoideum* dynein in the presence of ADP[93] (BOX 2). The nucleotide binds between the large and small subdomains of AAA1, interacting with several signature motifs (detailed in BOX 2). Moreover, in an intimate arrangement, the large subdomain of the adjacent module (AAA2) also contributes to the nucleotide-binding pocket of AAA1, providing an Arg finger that is crucial for ATP hydrolysis (BOX 2).

Comparison of *D. discoideum* and *S. cerevisiae* dynein motor structures in different nucleotide states supports the idea that large and small subdomains of AAA1 move relative to each other during the ATPase cycle. In the *D. discoideum* structure crystalized in the presence of ADP, AAA1 is partially closed around ADP, placing the backbone atoms of its Walker A and sensor II motifs ~13 Å apart[93] (BOX 2). In the *S. cerevisiae* structure crystalized in the absence of nucleotide, AAA1 is more open and the Walker A and sensor II motifs are ~17 Å apart. This open conformation of AAA1 cannot bind nucleotides following crystal soaking[95]. Thus, the open AAA1 conformer seen in the *S. cerevisiae* dynein structure seems to represent a state with very low affinity for nucleotide that is fixed by crystallization[95]. Free from the constraints of a crystal lattice, AAA1 is expected to bind and fully close around ATP, bringing the AAA2 Arg finger close enough to participate in hydrolysis and eliciting changes in the microtubule-binding domain and linker domain of dynein. In *D. discoideum* dynein, the products of ATP hydrolysis (P$_i$ and ADP) seem to be kinetically trapped in AAA1, based on pre-steady state studies[93]. The release of P$_i$ from AAA1 is stimulated by microtubules[93], suggesting that track binding might allosterically drive AAA1 towards the open conformation. In summary, current studies point to a model in which the opening and closing motions of AAA1 are the principal drivers of the mechanochemical cycle of dynein, coordinating its ATPase activity with microtubule binding and linker movement.

## Box 2 | The AAA+ engine

Each AAA+ module in the dynein ring contains a large subdomain (a five-stranded parallel β-sheet flanked by α-helices), which is flexibly joined to a smaller, predominantly α-helical, subdomain[93,95]. The small subdomain of AAA1 (AAA1s) packs against the large subdomain of AAA2 (AAA2L), and AAA2s packs against AAA3L, and so on, until the ring is closed by AAA6s packing against AAA1L (see the figure, part **a**). The highlighted subdomains are shown in detail for *Dictyostelium discoideum* dynein[93] (Protein Data Bank code: 3VKG) (see the figure, part **b**). AAA1 is the principal ATPase site and contains enzymatic motifs characteristic of the AAA+ superfamily. AAA1L bears Walker A and Walker B motifs, which are crucial for nucleotide binding and hydrolysis, respectively. Within the Walker A consensus sequence (Gly-Lys-Thr), the Lys residue (yellow) interacts with the phosphate groups of the nucleotide. Mutating this residue severely impairs nucleotide binding, thereby eliminating the motility of dynein while rendering it in a state that binds tightly to microtubules[85,100]. Within the Walker B sequence (Asp-Glu; at the end of the third β-strand), the Glu residue (green) is thought to be the catalytic base that polarizes $H_2O$ for an inline attack on the γ-phosphate of ATP[146]; mutating this residue to Gln severely impairs ATP hydrolysis and eliminates dynein motility[114]. However, ATP binding still occurs in the Walker B mutant, trapping dynein in an ATP-bound state with weak microtubule affinity and a primed linker domain[85,118]. AAA1L also contains a residue termed sensor I (typically Asp or Thr; not shown) that is implicated in hydrolysis[147]. AAA1s bears a residue termed sensor II (purple), an Arg residue that is thought to detect the status of the nucleotide pocket and help mediate closure of the AAA+ module in response to nucleotide binding (see the figure, part **c**). In addition, an Arg finger (orange) from AAA2L contributes to the ATPase site of AAA1. By analogy to other AAA+ proteins, this Arg finger is expected to be crucial for hydrolysis. In contrast to AAA1, the other AAA+ modules in the dynein ring show varying degrees of conservation with the enzymatic motifs of AAA+ superfamily members (Supplementary information S1 (table)). For example, across the dynein classes, AAA2 lacks the catalytic Walker B motif but contains a Walker A sequence, suggesting it can bind but not hydrolyse nucleotide. Consistent with this notion, when the *Saccharomyces cerevisiae* dynein motor is purified and crystallized in the absence of nucleotide, an ATP molecule seems to remain tightly bound in AAA2, further indicating that dissociation from this site is extremely slow[95].



*Nucleotide transactions at AAA2, AAA3 and AAA4.* In some AAA+ machines, such as the E1 helicase, ATP is thought to bind and hydrolyse in an ordered sequence around the ring[101]. In dynein, three AAA+ modules adjacent to AAA1 (AAA2, AAA3 and AAA4) can bind nucleotides, and the microtubule-binding stalk protrudes as an outgrowth of two α-helices in the small subdomain of AAA4. Thus, it could be envisioned that AAA1 and the stalk communicate via sequential nucleotide hydrolysis within AAA2–AAA4. However, structural and mutagenesis studies have ruled out this model. First, inspection of AAA2 indicates that it serves as a stable nucleotide-binding pocket rather than as an active site of hydrolysis (detailed in BOX 2). Second, eliminating nucleotide binding at AAA2 by mutagenesis slows down, rather than abrogates, dynein motility[100]. In dynein, long-lived nucleotide binding at AAA2 might keep this module in a comparatively rigid, closed conformation that is optimal for propagating structural changes to and from AAA1.

In most cytoplasmic dynein isoforms, AAA3 and AAA4 contain motifs indicative of active ATPase sites, but this is not the case in all dyneins (Supplementary information S1 (table)). For example, in IFT dynein, the catalytic Walker B motif in AAA3 is not well conserved[95]. Nevertheless, disabling nucleotide binding or hydrolysis at AAA3 in *D. discoideum* and *S. cerevisiae* cytoplasmic dynein severely slows motility; equivalent mutations in AAA4 have a milder effect[100,102]. In *D. discoideum* dynein, pre-steady state kinetic studies hint that AAA3 and AAA4 may spend most of their time in an ADP-bound state. When all other hydrolysis sites are disabled, both AAA3 and AAA4 release $P_i$ rapidly (~$60\,s^{-1}$) on mixing with ATP, then subsequently cycle at a lower rate (<$1\,s^{-1}$), probably owing to the slow release of ADP[93]. Unlike AAA1, these modules do not autonomously respond to microtubules[93]. However, it is an open question whether nucleotide turnover in AAA3 and AAA4 can be stimulated by the ATPase cycle of AAA1 (REF. 86). Alternatively, AAA3 and AAA4 might use hydrolysis principally to enter an ADP-bound state, perhaps giving these modules good geometry or appropriate flexibility to accommodate and propagate the motions of AAA1 in the ring. Interestingly, LIS1, a ubiquitous regulator of cytoplasmic dynein, engages the motor domain between AAA3 and AAA4 (REF. 103) and biases dynein towards a microtubule-bound state[103–105]. Whether LIS1 influences the ATPase activity of AAA3 and AAA4 is unknown.

*Functions of AAA5, AAA6 and the C-terminal region.* The two non-nucleotide-binding modules within the AAA+ ring, AAA5 and AAA6, share the same large–small subdomain architecture as the other AAA+ modules. However, AAA5 displays two distinct features. Two α-helices in its small subdomain are markedly elongated, forming the coiled-coil strut that interacts with the stalk[94,96] (FIG. 2c). The stalk and strut are extensions of different α-helices in AAA4 and AAA5, respectively, suggesting that they are not directly related[94,96]. AAA5 also bears an extension at its C-terminal end, comprising a compact bundle of α-helices, the role of which is not

yet clear[93]. Although AAA5 does not hydrolyse ATP, this does not mean it is a static component in the ring. Indeed, extrinsically driven opening and closing of AAA5, and associated angular shifts between the stalk and the strut, may be fundamental in coupling the ATPase cycle of AAA1 with microtubule binding (see below).

The ring is completed by the small subdomain of AAA6 packing against the large subdomain of AAA1. In addition, a structural element C-terminal to AAA6 is required for motor function. Comprising an α-helix that bridges the small subdomains of AAA5 and AAA6 (REF. 93,96), this structure would be expected to restrict motion within AAA6 if its position were maintained throughout the mechanochemical cycle[106], although this model remains untested. Such a role might be important for transmitting structural changes from AAA1 to AAA5 and the strut[93]. Most dyneins also possess a further C-terminal domain, which in *D. discoideum* consists of an incomplete β-barrel and several α-helices that spread out over AAA1, AAA5 and AAA6 (REF. 93). This C-terminal domain is not strictly required for movement and is absent in most fungal dyneins[83], but its truncation reduces the processivity of *D. discoideum* dynein dimers[107].

In summary, the global rearrangements within the dynein AAA+ ring and C-terminal sequence during the mechanochemical cycle are not yet clear. When thinking about how structural changes could propagate through the AAA+ ring, one approach is to mentally fix one segment of the ring and imagine the other segment (or segments) moving relative to this reference[93,94,96]. Alternatively, because the AAA+ ring is a topologically closed structure with six potential hinges, another perspective is that ATP binding and hinge closure in one of the AAA+ modules (for example AAA1) exerts strain on the rest of the ring[108], inducing the most compliant hinges (perhaps AAA5) to distort in response.

***Cyclic microtubule binding.*** For microtubule binding to stimulate the release of hydrolysis products from AAA1, a signal must be relayed from the microtubule-binding domain at the tip of the stalk to the AAA+ ring. An inverse pathway also operates, because ATP binding at AAA1 weakens the affinity of the microtubule-binding domain[85] (FIG. 3). Accumulating evidence suggests that the basis for transmitting signals to and from the microtubule-binding domain involves sliding between the outward (CC1) and return (CC2) α-helices in the stalk coiled coil, over a distance of 4.5–6 Å (equivalent to one turn along the α-helix). This model began with the deduction that the hydrophobic residues in CC1 and CC2 could potentially pack against each other in two types of registry, termed α- and β-registry, owing to an unusual heptad repeat in CC1 (REF. 109). Both registries have now been observed structurally: a specific β-registry (called +β-registry) in the context of a short stalk construct from mouse cytoplasmic dynein[110] and an α-registry within the entire *D. discoideum* dynein motor domain[93]. Moreover, fixing the stalk in different registries by protein engineering enforces distinct mechanochemical states. For example, the +β-registry confers weak microtubule

affinity[109–111] and low basal ATPase activity[111], whereas the α-registry confers strong microtubule affinity[109–111] and stimulates ATPase activity[111].

How might track binding cause the stalk to shift registry? Insight comes from a comparison of the mouse microtubule-binding domain in its weak binding state (visualized by crystallography[110]) versus its strong binding state on the microtubule (visualized by cryo-EM[112]). Notably, on forming a strong interface with the microtubule, an α-helix (known as H1) on the periphery of the microtubule-binding domain is displaced inwards (FIG. 4a,b). Because H1 directly attaches to CC1 in the stalk, such a movement could bias the coiled coil from the +β-registry towards the α-registry, as articulated in a pseudo-atomic model from electron microscopy and molecular dynamics analysis[112] (FIG. 4b). In the crystal structure of the complete *D. discoideum* motor, the stalk is in the α-registry, but the distal segment of CC1 is disordered and the microtubule-binding domain adopts the weak binding state[93]. These results suggest that the strong binding conformation may be critically stabilized by interactions with the microtubule[112], analogous to the situation with myosin 2 and actin[113].

The precise nature of helix sliding in the stalk is unclear. In one scenario, CC1 could move as a unit, undergoing a net translation and small rotation relative to CC2, although side chain rearrangements would be required to accommodate the new registry[109]. Alternatively, it is possible that CC1 moves by a reptation-like mechanism, in which a bulge propagates along the length of CC1 to generate the register change[110]. Although reptation would involve distortion along the CC1 backbone, analogous bulge propagation has been reported to occur in canonical coiled coils when strained using optical tweezers[114]. Furthermore, in the cryo-EM map of the dynein microtubule-binding domain in the α-registry[112], the coiled coil seems to open up near the microtubule surface (FIG. 4b), providing a potential site for bulge initiation.

Evidence suggests that the strut may transduce rearrangements in the stalk into enzymatic transitions in the AAA+ ring, and vice versa. When stalk–strut interactions are ablated via truncation of the strut, the ring displays an uncontrolled high ATPase rate in the absence or presence of microtubules[93]. As revealed by the *D. discoideum* dynein crystal structure, the strut forms an extensive interaction with the stalk in the α-registry, forming a four-helix bundle[93]. Specifically, the strut inserts three well-conserved Leu residues between CC1 and CC2 within the stalk (FIG. 4c). There is also a strikingly conserved triad of amino acids on CC2 of the stalk that forms a hydrogen bond interaction with an absolutely conserved Glu on the strut (FIG. 4c). How the stalk–strut interface changes during the mechanochemical cycle is unknown. One idea is that the strut might pivot on CC2 via this conserved triad, and this pivoting would couple with helix sliding or bulge formation in the stalk. In this model, angular shifts between the stalk and strut would be associated with the opening and closing of AAA5, which would feed back to AAA1 via the other AAA+ modules and the C-terminal sequence.

---

**E1 helicase**
A hexameric AAA+ ATPase protein from papillomavirus that encircles and translocates along single-stranded DNA, thereby unwinding DNA duplexes with a 3′ to 5′ directionality.

**Reptation**
Snake-like movement of a polymer along a path, originally introduced by De Gennes in the field of polymer theory.
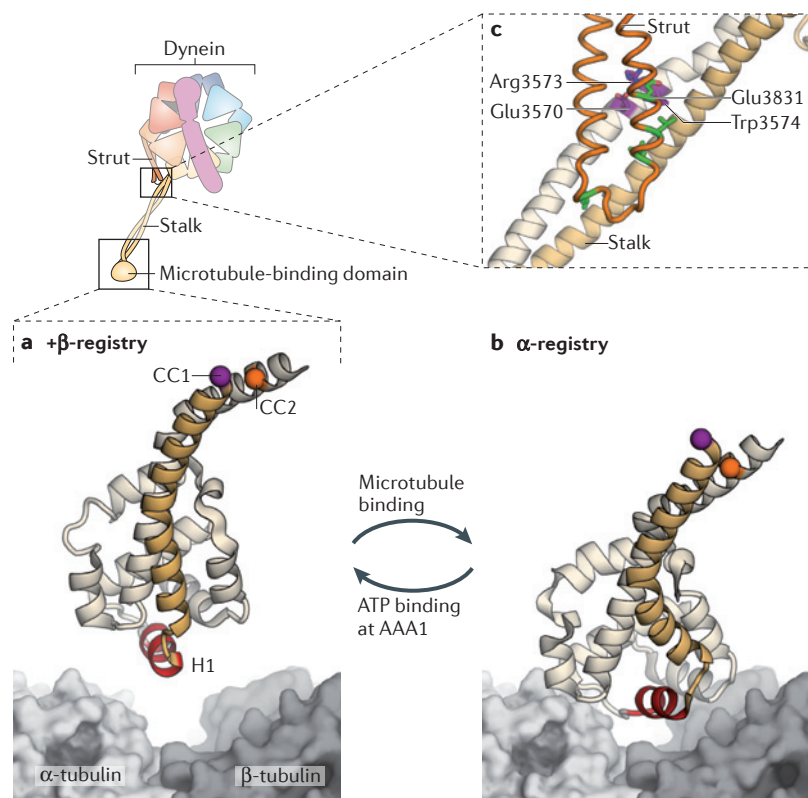
Figure 4 | **Cyclic microtubule binding.** A cartoon of the dynein motor domain is shown, with regions of interest enlarged in parts **a–c**. **a** | Crystal structure of the microtubule-binding domain from mouse cytoplasmic dynein in its weak binding state[110] (Protein Data Bank (PDB) code: 3ERR), shown above a surface representation of a tubulin dimer. **b** | Model of the mouse microtubule-binding domain strongly bound to the tubulin dimer, based on a ~10 Å cryo-electron microscopy (cryo-EM) map and steered molecular dynamics[112] (PDB code: 3J1T). The binding site of dynein between α-tubulin and β-tubulin overlaps with that of kinesin[149]. Although the positioning of atoms in the cryo-EM derived model of the microtubule-binding domain is less certain than in the crystal structure, it is clear that helix H1 undergoes a large displacement on forming a strong interface with the microtubule[112]. Movement of H1 is thought to be associated with changes in the relative alignment or registry of the α-helices (CC1 and CC2) of the stalk, thereby allowing the microtubule-binding domain and the AAA+ ring to communicate through the stalk. This communication is vital for dynein movement, as it allows the microtubule-binding domain to sequentially bind and release its track during the ATPase cycle (see FIG. 3). A marker on CC1 (purple) and CC2 (orange) is coloured in each panel to highlight the registry change between the models. **c** | Communication between the AAA+ ring and the microtubule-binding domain depends critically[93] on interactions between the stalk (an outgrowth of AAA4) and the strut (an outgrowth of AAA5). These stalk–strut interactions are expected to change during the ATPase cycle but, thus far, they have only been visualized in the ADP-bound state of the *Dictyostelium discoideum* dynein motor, in which the stalk adopts the α-registry[93]. Four highly conserved residues on the strut (Glu3831, Leu3835, Leu3838 and Leu3846; green) and a highly conserved triad of residues on CC2 of the stalk (Glu3570, Arg3573 and Trp3574; purple) might be important for the structure and dynamics of the stalk–strut interface.

Finally, electron microscopy studies indicate that the stalk is a compliant element, capable of flexing with respect to the rest of the motor domain[91,92,115]. Reinforcing this view of the stalk as a somewhat flexible entity, the two copies of the *D. discoideum* dynein motor domain in the crystallographic asymmetric unit display different stalk angles[93], and the packing between CC1 and CC2 differs between these 'fleximers' (REF. 115). The compliance of the stalk is an intriguing property for a structure that must

also transmit subtle conformational changes and sustain force between dynein and the microtubule[116]. In fact, it is possible that these activities are closely coupled, as strain on the stalk could conceivably influence the registry between CC1 and CC2 and hence alter the affinity of the microtubule-binding domain. In this regard, it is notable that *S. cerevisiae* cytoplasmic dynein shows an asymmetric response to load, with more force being required to pull it backwards (towards the microtubule plus end) than forwards (towards the minus end)[117].

*Remodelling of the linker.* Arching over the AAA+ ring is the linker domain — the main mechanical element of dynein (FIG. 2c). It is 10 years since the linker was discovered by electron microscopy and proposed to be the principal structure that amplifies conformational changes in the AAA+ modules[92]. This model has garnered support from 2D and 3D electron microscopy studies of axonemal and cytoplasmic dyneins[90–92], as well as from fluorescence resonance energy transfer (FRET)[118] and dynein motility assays[83,119]. However, the full extent of the functions of the linker is still emerging. Structurally, the linker comprises five subdomains that form an elongated rod[93,95] (FIG. 5a). The C-terminal end forms an extensive interface with the ring, chiefly involving the large subdomain of AAA1. The N-terminal end of the linker undergoes large-scale movements during the ATPase cycle[90–92,118] that are crucial for transmitting force to the tail and attached cargo[83,119] (FIG. 3).

The question of how the linker moves is therefore key to understanding dynein as a force-generating machine. Several lines of evidence now point towards a model in which the linker is remodelled by interactions with the AAA+ ring. As noted in crystallographic studies, a cleft exists within the linker, suggestive of a hinge[93,95,96] (FIG. 5a). However, spontaneous sharp bending about this cleft does not seem to occur readily. When the linker is detached or 'undocked' from the AAA+ ring (via a C-terminal truncation that destabilizes *D. discoideum* dynein), the linker retains a rather stable straight form in most molecules, as revealed by electron microscopy and image processing[90] (FIG. 5a). Insights into what promotes or stabilizes bending of the linker come from the *D. discoideum* dynein crystal structure in the ADP-bound state[93]. Within the large subdomain of AAA2, there are two β-hairpin inserts (the pre-sensor-I (PS-I) and helix 2 (H2) inserts), which contact the linker near the cleft (FIG. 5a). On exchange of ADP for ATP, full closure of AAA1 might bring these inserts into a closer embrace with the linker to elicit bending and/or to stabilize the bent conformation[93,95] (FIG. 5b). EM studies indicate that when ATP or ADP.Vi (ADP plus vanadate, a phosphate analogue) are bound to AAA1, the distal linker is bent towards AAA2 in most molecules (FIG. 5b,c) but remains straight in a subpopulation[90,91]. This raises the possibility that linker remodelling is an equilibrium process that is biased by ATP binding, rather than a switch-like transition. It is anticipated that a high-resolution crystal structure of dynein with ATP or an analogue bound to AAA1 will clarify how the linker is remodelled. Moreover, because such a structure may represent a snapshot of a fluctuating state, it will need to be combined with

experiments that can reveal the dynamics of the linker to gain a full understanding of the remodelling reaction.

With the linker bent towards AAA2, binding of the motor to the microtubule is thought to stimulate $P_i$ release and trigger the powerstroke, in which the linker straightens to lie over AAA4 (FIG. 5c). This path would take the linker over AAA3; whether there is interplay between the linker and the nucleotide status of AAA3 or AAA4 is unknown. During the powerstroke transition, the end of the linker would move principally along the long axis of the stalk[91], and it has been posited that the angle at which the stalk binds the microtubule is an important determinant of the directionality of the powerstroke[110]. Consistent with this idea, various dyneins have
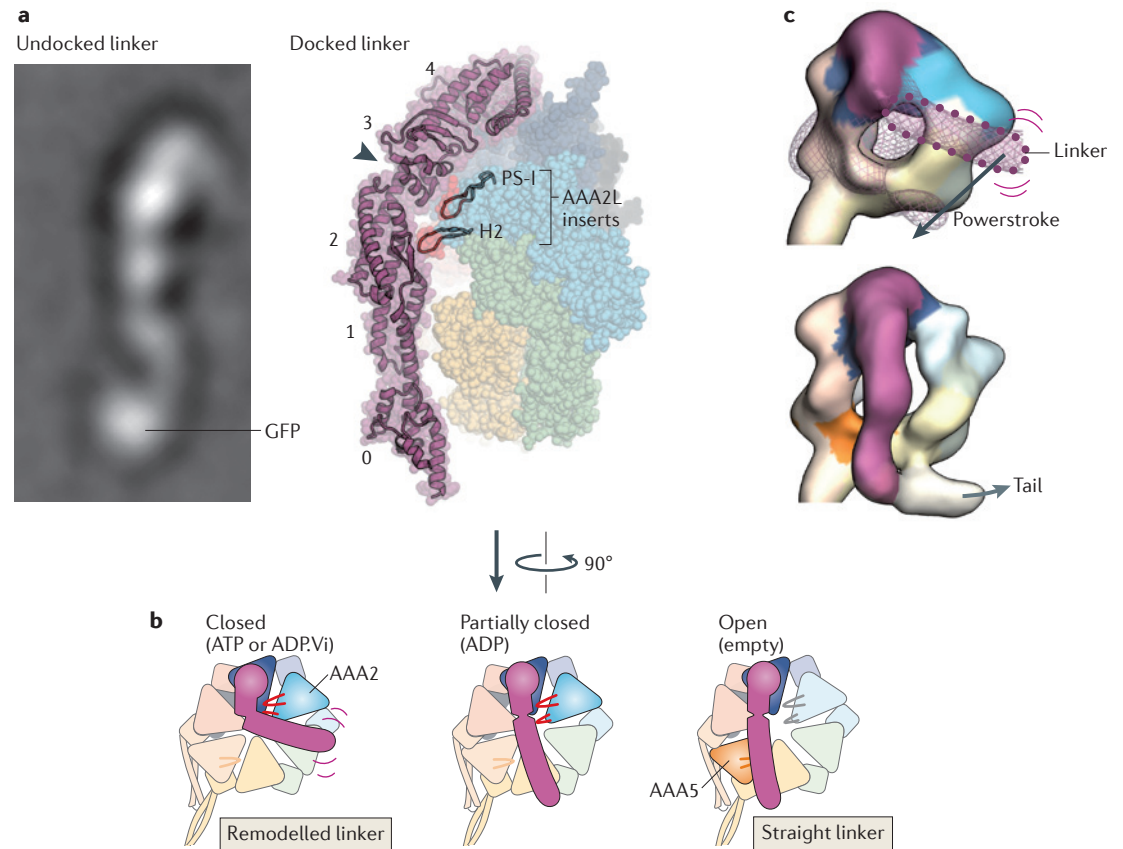


Figure 5 | **Linker domain structure and remodelling.** Rearrangements in the linker domain's structure are crucial for dynein motility. **a** | Electron microscopy image of the linker domain from *Dictyostelium discoideum* dynein when it is undocked from the AAA+ ring, showing that the linker is a stable structural entity (left). A GFP tag on the amino-terminal end of the linker is labelled. Linker undocking has, thus far, been observed by electron microscopy only in purified dyneins[90–92], and it is not known whether it can occur under physiological settings. View of the linker arching over the AAA+ ring in the *D. discoideum* dynein crystal structure in the ADP-bound state[93] (right). The five subdomains in the linker are numbered (0–4). The cleft between subdomains 2 and 3, which is spanned by a single α-helix, is indicated by the arrowhead. Two β-hairpin inserts (PS-I and H2) within the large subdomain of AAA2 (AAA2L) that contact the linker near the cleft are highlighted. In addition to the cleft, note that there is a tenuous connection between linker subdomains 0 and 1 that could potentially deform, for example, under strain. **b** | Model of linker remodelling based on available structural data[90–93,95,118]. When ATP or ADP.Vi (ADP plus vanadate) is bound in AAA1, the linker seems to be mobile (indicated by purple lines) but bent towards AAA2 in most molecules, according to cryo-EM studies of *Chlamydomonas reinhardtii* inner arm dynein-c and *D. discoideum* cytoplasmic dynein[90] (left). The PS-I and H2 inserts in AAA2 (shown in red) are strong candidates to mediate this remodelling of the linker[93,95]. Following inorganic phosphate ($P_i$) release, the linker is thought to undergo a powerstroke, in which it straightens to lie over AAA4, based on the *D. discoideum* dynein crystal structure[93] (middle). AAA1 is partially closed around ADP, and the PS-I and H2 inserts form a limited interaction with the linker. Finally, the linker docks at AAA5, as has been observed for *Saccharomyces cerevisiae* cytoplasmic dynein and *C. reinhardtii* inner arm dynein-c in the absence of nucleotide (right). This step is proposed to fully open AAA1 and thus eject ADP[95]. It is unknown if the inserts within the core folds of AAA3 and AAA4 (not shown) can also interact with the linker[106]. **c** | Cryo-electron microscopy maps of *C. reinhardtii* inner arm dynein-c in the ADP.Vi-bound state (upper) and in the absence of nucleotide (lower)[90] (Electron Microscopy Data Bank codes: 2156 and 2155, respectively). The maps are coloured as in part **b**, with AAA+ modules interacting with the linker shown in saturated colours and other modules in pale colours. In the ADP.Vi map, density for the distal linker is missing, owing to variability in its position. The position of the distal linker suggested by a variance map (purple wiremesh) and GFP-based tagging is shown with a dotted outline[90]. Straightening of the linker is thought to represent the powerstroke of dynein (FIG. 3). Electron microscopy image in part **a** courtesy of B. Malkova, Biomolecular Research Laboratory, Paul Scherrer Institute, Switzerland.

been shown to bind preferentially with the stalk angled from the ring towards the microtubule minus end — the direction of dynein movement[110,112,120,121] (FIG. 2c).

The linker can also influence enzymatic transitions within the AAA+ ring. Small N-terminal truncations and mutations within the linker impair the ATPase activity and motility of dynein, although the precise functional boundary may differ between species[83,89,91,95]. When *S. cerevisiae* cytoplasmic dynein and *C. reinhardtii* inner arm dynein-c are visualized in the nucleotide-free state, the N-terminal region of the linker forms a contact with the large subdomain of AAA5 (REFS 90,95) (FIG. 5b). This differs from the ADP-bound *D. discoideum* dynein structure[93], in which the linker lies above AAA4 (FIG. 5b). It has been proposed that, by shifting to interact with AAA5, the linker may function as a spacer that applies tension to the AAA+ ring, prying open AAA1 and promoting ADP release after the powerstroke[95]. Similarly, it is possible that rearward strain on the linker (imparted by cargo or a partnering motor domain) could favour the closed conformation of AAA1, thus inhibiting ADP release and microtubule detachment. In summary, the linker domain may have functions beyond delivering the powerstroke of dynein, such as sensing strain and regulating progression through the mechanochemical cycle.

## Emergent motile properties

According to the model in FIG. 3, a single dynein motor domain would bind to the microtubule, perform a solitary tug and then diffuse away after binding ATP[103]. However, when multiple dynein motor domains act together, as is typical in living cells, striking additional motile behaviours can emerge. One example is the beating motions of cilia, which are driven by the thousands of dyneins within the axoneme (BOX 1). Another is the processive motion produced by cytoplasmic dynein dimers.

When two *S. cerevisiae* cytoplasmic dynein motor domains are paired (either naturally via the tail or by fusing an exogenous dimerizing moiety to the end of the linker), the resulting dimer can move along the microtubule for ~1,500 nm before detaching, as revealed by *in vitro* single-molecule studies[83,122]. These movements represent dozens of individual steps, with each motor domain typically moving in 8–16 nm increments[83,122,123], corresponding to a distance of 1–2 tubulin dimers along the long axis of the microtubule. Larger steps, as well as sideways and backwards excursions, are also observed, suggesting there is a diffusive component to each step[83,122,123]. Furthermore, optical trapping has revealed that *S. cerevisiae* cytoplasmic dynein dimers are high-force motors, capable of moving against resisting loads of up to 7 pN before stalling[117].

By labelling each motor domain with a different coloured fluorophore, the relative movements within the *S. cerevisiae* dimer have recently been unveiled[122,123]. Remarkably, there is no strict pattern to the steps: the motor domains do not need to alternately pass each other in space and, in some cases, the rear motor can take multiple steps while the lead motor remains stationary, and vice versa. This contrasts with the methodical 'hand-over-hand' movements of kinesin 1 and myosin 5 dimers,

which arise from alternating ATPase cycles in their motor domains[9]. In the case of the less rigid stepping pattern of dynein, what prevents both motor domains detaching from the microtubule simultaneously? One part of the answer may lie in the duty ratio of the *S. cerevisiae* motor domain[122,123] (that is, the fraction of the mechanochemical cycle spent attached to the track). This parameter has not been measured for *S. cerevisiae* dynein but, as a theoretical example, if the motor domains acted independently but spent 90% of their cycle attached to the microtubule, the dimer would still be expected to take ~70 steps on average before detaching[124]. Yet, a purely stochastic model does not capture all of the features of the stepping behaviour in *S. cerevisiae* dynein. Notably, as the separation between the motor domains along the microtubule increases, the probability of the rear head taking a step becomes greater and the stepping of the lead head is inhibited[122,123]. It has been proposed that this reflects a response of the motor domains to internal strain within the dimer[122,123]. Whether this strain sensing is mediated via the stalk, the linker or some other unknown mechanism awaits discovery.

Interestingly, in *D. discoideum* cytoplasmic dynein, the two motor domains may influence one another's enzymatic cycles more strongly. In this system, the intrinsic duty ratio of each motor domain is low (24%)[125]. Thus, in the absence of any communication, the dimer would be expected to take only around two steps along the microtubule on average before detaching[124] — at odds with the measured run length of ~750 nm[107]. Moreover, following dimerization, the ATPase rate of the *D. discoideum* motor domain on the microtubule is slowed down by ~70%, further pointing towards enzymatic regulation within the dimer[107]. Elucidating the basis for this intra-dimer communication will require structural information on the geometry of *D. discoideum* dynein dimers on the microtubule, coupled with two-colour tracking of each motor domain. In summary, the mechanism and extent of communication within cytoplasmic dynein dimers from different species is an active area of research.

## Conclusions and perspectives

Fifty years since the discovery of its founding member, the dynein family is now known to participate in a broad range of cellular functions involving microtubule-based movement. A model for the basic reaction of dynein with the microtubule is beginning to emerge from mechanistic studies on its motor domain, but crucial features remain untested. Some concepts, such as the motions of AAA1 and the use of inserts in the AAA+ modules to remodel the linker domain, are reminiscent of the actions of other AAA+ mechanoenzymes. However, other aspects of the dynein mechanism, such as the interplay between the stalk, strut and microtubule, are without precedent.

The roles of the subsidiary nucleotide-binding modules of dynein, particularly AAA3 and AAA4, remain mysterious. New tools, perhaps involving module-specific conformation sensors[126], are needed to elucidate their function. Simultaneous visualization of stepping and nucleotide binding, as has been achieved for myosin 5 (REF. 127), would be highly informative. We can also

# REVIEWS

look forward to high-resolution structures of dynein in different nucleotide states, which might clarify how small changes in the active site of AAA1 are propagated through the large dynein motor domain. Simulations and experiments are required to test exactly how the α-helices of the stalk slide relative to one another. And small-molecule inhibitors (such as ciliobrevin[128]) may be useful in trapping specific conformational states of the motor, as well as in unravelling the cellular functions of dynein.

Our current picture of dynein motility is a synthesis of data from various dynein species and truncated constructs, in part owing to the challenges associated with working with intact dynein holoenzymes. However, it will be important to elucidate how dynein holoenzymes work and how they have diverged from one another to carry out specific biological functions. Ciliary beating, for example, arises from the action of numerous dynein species, each with distinct motile characteristics[129]. It is known that a subset of inner arm dyneins can rotate microtubules around their long axis as they translocate them in *in vitro* assays[130] and that some have specialized structural features such as curved stalk domains[92], but how these properties relate to ciliary motility is unclear at present.

There is also much to learn about variations in the behaviour of cytoplasmic dynein. For instance, one controversial area is the force produced by a single mammalian cytoplasmic dynein complex. Although several studies have measured a stall force of ~1 pN[104,131–133], reports of higher stall forces of 5–7 pN persist[134,135]. Does this discrepancy arise from differences in protein handling? Or are there subpopulations of cytoplasmic dynein *in vivo* with distinct force-producing capacities that are isolated by different purification methods? Answers to these questions are keenly sought, and they have the potential to provide insights into how dynein is regulated in the cell. In contrast to previous studies with tissue-purified dynein, a recent study using recombinant protein challenges the idea that mammalian cytoplasmic dynein complexes are intrinsically processive, indicating that additional factors could be required for sustained movement[27]. There are also reports that mammalian cytoplasmic dynein has the ability to move towards the plus end of the microtubule[135,136], although the structural and

mechanistic basis for this behaviour remains unknown. Very little is known about the motility of IFT dynein and how it is adapted for IFT.

Looking forward, we anticipate a more complete fusion of cell biological and *in vitro* analyses of dynein. One challenge will be bringing the high precision of *in vitro* measurements to single dynein molecules, regulators and cargoes in living cells, but important advances are being made in this area. For example, a recent study was able to track single cytoplasmic dynein molecules within the *Schizosaccharomyces pombe* cell volume using highly inclined and laminated optical sheet microscopy[137], and in-cell optical trapping is revealing the force-producing behaviour of cargo-bound motors *in situ*[80]. Fungi have been, and will continue to be, powerful model systems for studying intracellular transport, in part because genes of interest can be readily tagged and modified at their genomic loci. Advances in genome editing technologies should make it easier to perform similar manipulations on the dynein machinery in metazoan cells. And, to complement the insights from living cells, another important challenge will be to reconstitute more complex dynein-powered motile systems *in vitro* using purified proteins. Analysis of cell extracts, which combine near-cellular complexity with biochemical tractability, offers an interesting way to help bridge the gap between *in vivo* and *in vitro* studies.

Finally, structural information will have an important part to play in uncovering how dyneins are harnessed in cells. A high-resolution structure of the dynein tail domain with its associated subunits is expected to shed light on how dyneins oligomerize and engage cargo. Insight into the architecture of the dynein–dynactin complex and other regulatory assemblies will be essential. Moreover, at intermediate resolution, cryo-EM and tomography have the potential to visualize the arrangement of the two motor domains of cytoplasmic dynein on the microtubule, as well as how groups of motors self-organize on macromolecular cargo. Combining such structural data with dynamic information from *in vitro* and *in vivo* studies promises to reveal the workings of dyneins in breathtaking detail, sufficient to understand their dysfunction in disease and perhaps design synthetic applications for dynein.

1. Moughamian, A. J. & Holzbaur, E. in *Dyneins: Structure, Biology and Disease* (ed. King, S. M) 584–601 (Elsevier Inc., 2011).
2. Fliegauf, M., Benzing, T. & Omran, H. When cilia go bad: cilia defects and ciliopathies. *Nature Rev. Mol. Cell Biol.* **8**, 880–893 (2007).
3. Gibbons, I. R. Studies on the protein components of cilia from *Tetrahymena pyriformis*. *Proc. Natl Acad. Sci. USA* **50**, 1002–1010 (1963).
4. Gibbons, I. & Rowe, A. Dynein: a protein with adenosine triphosphatase activity from cilia. *Science* **149**, 424–426 (1965).
   **References 3 and 4 mark the discovery of dynein motor proteins.**
5. Paschal, B. M., Shpetner, H. S. & Vallee, R. B. MAP 1C is a microtubule-activated ATPase which translocates microtubules *in vitro* and has dynein-like properties. *J. Cell Biol.* **105**, 1273–1282 (1987).
   **Describes the isolation and characterization of cytoplasmic dynein.**
6. Paschal, B. M. & Vallee, R. B. Retrograde transport by the microtubule-associated protein MAP 1C. *Nature* **330**, 181–183 (1987).

7. Schroer, T. A., Steuer, E. R. & Sheetz, M. P. Cytoplasmic dynein is a minus end-directed motor for membranous organelles. *Cell* **56**, 937–946 (1989).
8. Vale, R. D., Reese, T. S. & Sheetz, M. P. Identification of a novel force-generating protein, kinesin, involved in microtubule-based motility. *Cell* **42**, 39–50 (1985).
9. Vale, R. D. & Milligan, R. A. The way things move: looking under the hood of molecular motor proteins. *Science* **288**, 88–95 (2000).
10. Billington, N. & Sellers, J. R. Dynein struts its stuff. *Nature Struct. Mol. Biol.* **18**, 635–636 (2011).
11. Neuwald, A. F., Aravind, L., Spouge, J. L. & Koonin, E. V. AAA + : a class of chaperone-like ATPases associated with the assembly, operation, and disassembly of protein complexes. *Genome Res.* **9**, 27–43 (1999).
12. Vallee, R. B., McKenney, R. J. & Ori-McKenney, K. M. Multiple modes of cytoplasmic dynein regulation. *Nature Cell Biol.* **14**, 224–230 (2012).
13. Kardon, J. & Vale, R. Regulators of the cytoplasmic dynein motor. *Nature Rev. Mol. Cell Biol.* **10**, 854–865 (2009).

14. Allan, V. J. Cytoplasmic dynein. *Biochem. Soc. Trans.* **39**, 1169–1178 (2011).
15. Akhmanova, A. & Hammer, J. A. 3rd. Linking molecular motors to membrane cargo. *Curr. Opin. Cell Biol.* **22**, 479–487 (2010).
16. Riedel-Kruse, I. H., Hilfinger, A., Howard, J. & Jülicher, F. How molecular motors shape the flagellar beat. *HFSP J.* **1**, 192–208 (2007).
17. Brokaw, C. Thinking about flagellar oscillation. *Cell. Motil. Cytoskeleton* **66**, 425–436 (2009).
18. Lindemann, C. B. & Lesich, K. A. Flagellar and ciliary beating: the proven and the possible. *J. Cell Sci.* **123**, 519–528 (2010).
19. King, S. M. Integrated control of axonemal dynein AAA+ motors. *J. Struct. Biol.* **179**, 222–228 (2012).
20. Wickstead, B. & Gull, K. Dyneins across eukaryotes: a comparative genomic analysis. *Traffic* **8**, 1708–1721 (2007).
21. Vale, R. D. The molecular motor toolbox for intracellular transport. *Cell* **112**, 467–480 (2003).
22. Yagi, T. Bioinformatic approaches to dynein heavy chain classification. *Methods Cell Biol.* **92**, 1–9 (2009).

23. Moore, J., Stuchell-Brereton, M. & Cooper, J. Function of dynein in budding yeast: mitotic spindle positioning in a polarized cell. *Cell. Motil. Cytoskeleton* **66**, 546–555 (2009).

24. Egan, M. J., McClintock, M. A. & Reck-Peterson, S. L. Microtubule-based transport in filamentous fungi. *Curr. Opin. Microbiol.* **15**, 637–645 (2012).

25. Koonce, M. P. Dictyostelium, a model organism for microtubule-based transport. *Protist* **151**, 17–25 (2000).

26. Pfister, K. K. *et al.* Genetic analysis of the cytoplasmic dynein subunit families. *PLoS Genet.* **2**, e1 (2006).

27. Trokter, M., Mücke, N. & Surrey, T. Reconstitution of the human cytoplasmic dynein complex. *Proc. Natl Acad. Sci. USA* **109**, 20895–20900 (2012).
    **Describes the reconstitution of the human cytoplasmic dynein complex from recombinant subunits. Surprisingly, despite driving robust microtubule gliding, the complexes do not show processive motility, suggesting that additional factors might be required for this behaviour.**

28. Schroer, T. A. Dynactin. *Annu. Rev. Cell Dev. Biol.* **20**, 759–779 (2004).

29. Driskell, O. J., Mironov, A., Allan, V. J. & Woodman, P. G. Dynein is required for receptor sorting and the morphogenesis of early endosomes. *Nature Cell Biol.* **9**, 113–120 (2007).

30. Jordens, I. *et al.* The Rab7 effector protein RILP controls lysosomal transport by inducing the recruitment of dynein-dynactin motors. *Curr. Biol.* **11**, 1680–1685 (2001).

31. Blocker, A. *et al.* Molecular requirements for bi-directional movement of phagosomes along microtubules. *J. Cell Biol.* **137**, 113–129 (1997).

32. Gross, S. P. *et al.* Interactions and regulation of molecular motors in *Xenopus* melanophores. *J. Cell Biol.* **156**, 855–865 (2002).

33. Kural, C. *et al.* Kinesin and dynein move a peroxisome *in vivo*: a tug-of-war or coordinated movement? *Science* **308**, 1469–1472 (2005).

34. Gross, S. P., Welte, M. A., Block, S. M. & Wieschaus, E. F. Dynein-mediated cargo transport *in vivo*. A switch controls travel distance. *J. Cell Biol.* **148**, 945–956 (2000).

35. Pilling, A. D., Horiuchi, D., Lively, C. M. & Saxton, W. M. Kinesin-1 and dynein are the primary motors for fast transport of mitochondria in *Drosophila* motor axons. *Mol. Biol. Cell* **17**, 2057–2068 (2006).

36. Presley, J. F. *et al.* ER-to-Golgi transport visualized in living cells. *Nature* **389**, 81–85 (1997).

37. Heerssen, H. M., Pazyra, M. F. & Segal, R. A. Dynein motors transport activated Trks to promote survival of target-dependent neurons. *Nature Neurosci.* **7**, 596–604 (2004).

38. Young, A., Dictenberg, J. B., Purohit, A., Tuft, R. & Doxsey, S. J. Cytoplasmic dynein-mediated assembly of pericentrin and gamma tubulin onto centrosomes. *Mol. Biol. Cell* **11**, 2047–2056 (2000).

39. Harrell, J. M. *et al.* Evidence for glucocorticoid receptor transport on microtubules by dynein. *J. Biol. Chem.* **279**, 54647–54654 (2004).

40. Shah, J. V., Flanagan, L. A., Janmey, P. A. & Leterrier, J. F. Bidirectional translocation of neurofilaments along microtubules mediated in part by dynein/dynactin. *Mol. Biol. Cell* **11**, 3495–3508 (2000).

41. Wilkie, G. S. & Davis, I. *Drosophila* wingless and pair-rule transcripts localize apically by dynein-mediated transport of RNA particles. *Cell* **105**, 209–219 (2001).

42. Johnston, J. A., Illing, M. E. & Kopito, R. R. Cytoplasmic dynein/dynactin mediates the assembly of aggresomes. *Cell. Motil. Cytoskeleton* **53**, 26–38 (2002).

43. Maday, S., Wallace, K. E. & Holzbaur, E. L. F. Autophagosomes initiate distally and mature during transport toward the cell soma in primary neurons. *J. Cell Biol.* **196**, 407–417 (2012).

44. Dodding, M. P. & Way, M. Coupling viruses to dynein and kinesin-1. *EMBO J.* **30**, 3527–3539 (2011).

45. Sato, A. *et al.* Cytoskeletal forces span the nuclear envelope to coordinate meiotic chromosome pairing and synapsis. *Cell* **139**, 907–919 (2009).

46. Steinberg, G. *et al.* Motor-driven motility of fungal nuclear pores organizes chromosomes and fosters nucleocytoplasmic transport. *J. Cell Biol.* **198**, 343–355 (2012).

47. Schnyder, T. *et al.* B cell receptor-mediated antigen gathering requires ubiquitin ligase Cbl and adaptors Grb2 and Dok-3 to recruit dynein to the signaling microcluster. *Immunity* **34**, 905–918 (2011).

48. Hashimoto-Tane, A. *et al.* Dynein-driven transport of T cell receptor microclusters regulates immune synapse formation and T cell activation. *Immunity* **34**, 919–931 (2011).

49. Laan, L. *et al.* Cortical dynein controls microtubule dynamics to generate pulling forces that position microtubule asters. *Cell* **148**, 502–514 (2012).

50. Hendricks, A. G. *et al.* Dynein tethers and stabilizes dynamic microtubule plus ends. *Curr. Biol.* **22**, 632–637 (2012).

51. Tsai, J.-W., Bremner, K. H. & Vallee, R. B. Dual subcellular roles for LIS1 and dynein in radial neuronal migration in live brain tissue. *Nature Neurosci.* **10**, 970–979 (2007).

52. Dujardin, D. L. *et al.* A role for cytoplasmic dynein and LIS1 in directed cell movement. *J. Cell Biol.* **163**, 1205–1211 (2003).

53. Combs, J. *et al.* Recruitment of dynein to the Jurkat immunological synapse. *Proc. Natl Acad. Sci. USA* **103**, 14883–14888 (2006).

54. McNally, F. J. Mechanisms of spindle positioning. *J. Cell Biol.* **200**, 131–140 (2013).

55. Kiyomitsu, T. & Cheeseman, I. M. Chromosome- and spindle-pole-derived signals generate an intrinsic code for spindle position and orientation. *Nature Cell Biol.* **14**, 311–317 (2012).

56. Collins, E. S., Balchand, S. K., Faraci, J. L., Wadsworth, P. & Lee, W.-L. Cell cycle-regulated cortical dynein/dynactin promotes symmetric cell division by differential pole motion in anaphase. *Mol. Biol. Cell* **23**, 3380–3390 (2012).

57. Mitchison, T. *et al.* Growth, interaction, and positioning of microtubule asters in extremely large vertebrate embryo cells. *Cytoskeleton (Hoboken)* **69**, 738–750 (2012).

58. Kimura, K. & Kimura, A. Intracellular organelles mediate cytoplasmic pulling force for centrosome centration in the *Caenorhabditis elegans* early embryo. *Proc. Natl Acad. Sci. USA* **108**, 137–142 (2011).

59. Longoria, R. A. & Shubeita, G. T. Cargo transport by cytoplasmic dynein can center embryonic centrosomes. *PLoS ONE* **8**, e67710 (2013).

60. Corthesy-Theulaz, I., Pauloin, A. & Pfeffer, S. R. Cytoplasmic dynein participates in the centrosomal localization of the Golgi complex. *J. Cell Biol.* **118**, 1333–1345 (1992).

61. Levy, J. R. & Holzbaur, E. L. Dynein drives nuclear rotation during forward progression of motile fibroblasts. *J. Cell Sci.* **121**, 3187–3195 (2008).

62. Raaijmakers, J. A. *et al.* Nuclear envelope-associated dynein drives prophase centrosome separation and enables Eg5-independent bipolar spindle formation. *EMBO J.* **31**, 4179–4190 (2012).

63. Salina, D. *et al.* Cytoplasmic dynein as a facilitator of nuclear envelope breakdown. *Cell* **108**, 97–107 (2002).

64. Heald, R. *et al.* Self-organization of microtubules into bipolar spindles around artificial chromosomes in *Xenopus* egg extracts. *Nature* **382**, 420–425 (1996).

65. Merdes, A., Ramyar, K., Vechio, J. D. & Cleveland, D. W. A complex of NuMA and cytoplasmic dynein is essential for mitotic spindle assembly. *Cell* **87**, 447–458 (1996).

66. Foley, E. A. & Kapoor, T. M. Microtubule attachment and spindle assembly checkpoint signalling at the kinetochore. *Nature Rev. Mol. Cell Biol.* **14**, 25–37 (2012).

67. Howell, B. J. *et al.* Cytoplasmic dynein/dynactin drives kinetochore protein transport to the spindle poles and has a role in mitotic spindle checkpoint inactivation. *J. Cell Biol.* **155**, 1159–1172 (2001).

68. Wojcik, E. *et al.* Kinetochore dynein: its dynamics and role in the transport of the Rough deal checkpoint protein. *Nature Cell Biol.* **3**, 1001–1007 (2001).

69. Varma, D., Monzo, P., Stehman, S. A. & Vallee, R. B. Direct role of dynein motor in stable kinetochore–microtubule attachment, orientation, and alignment. *J. Cell Biol.* **182**, 1045–1054 (2008).

70. Yang, Z., Tulu, U. S., Wadsworth, P. & Rieder, C. L. Kinetochore dynein is required for chromosome motion and congression independent of the spindle checkpoint. *Curr. Biol.* **17**, 973–980 (2007).

71. Ishikawa, H. & Marshall, W. F. Ciliogenesis: building the cell's antenna. *Nature Rev. Mol. Cell Biol.* **12**, 222–234 (2011).

72. Pazour, G. J., Dickert, B. L. & Witman, G. B. The DHC1b (DHC2) isoform of cytoplasmic dynein is required for flagellar assembly. *J. Cell Biol.* **144**, 473–481 (1999).

73. Porter, M. E., Bower, R., Knott, J. A., Byrd, P. & Dentler, W. Cytoplasmic dynein heavy chain 1b is required for flagellar assembly in *Chlamydomonas*. *Mol. Biol. Cell* **10**, 693–712 (1999).

74. Mikami, A. *et al.* Molecular structure of cytoplasmic dynein 2 and its distribution in neuronal and ciliated cells. *J. Cell Sci.* **115**, 4801–4808 (2002).

75. Perrone, C. A. *et al.* A novel dynein light intermediate chain colocalizes with the retrograde motor for intraflagellar transport at sites of axoneme assembly in *Chlamydomonas* and mammalian cells. *Mol. Biol. Cell* **14**, 2041–2056 (2003).

76. Ichikawa, M., Watanabe, Y., Murayama, T. & Toyoshima, Y. Y. Recombinant human cytoplasmic dynein heavy chain 1 and 2: observation of dynein-2 motor activity *in vitro*. *FEBS Lett.* **585**, 2419–2423 (2011).

77. Pigino, G. *et al.* Electron-tomographic analysis of intraflagellar transport particle trains *in situ*. *J. Cell Biol.* **187**, 135–148 (2009).

78. Laib, J. A., Marin, J. A., Bloodgood, R. A. & Guilford, W. H. The reciprocal coordination and mechanics of molecular motors in living cells. *Proc. Natl Acad. Sci. USA* **106**, 3190–3195 (2009).

79. Shih, S. M. *et al.* Intraflagellar transport drives flagellar surface motility. *Elife* **2**, e00744 (2013).

80. Mallik, R., Rai, A. K., Barak, P., Rai, A. & Kunwar, A. Teamwork in microtubule motors. *Trends Cell Biol.*, http://dx.doi.org/10.1016/j.tcb.2013.06.003 (2013).

81. Koonce, M. P. & Samsó, M. Overexpression of cytoplasmic dynein's globular head causes a collapse of the interphase microtubule network in Dictyostelium. *Mol. Biol. Cell* **7**, 935–948 (1996).
    **Details a recombinant expression system for the *D. discoideum* cytoplasmic dynein motor domain, forming the foundation for numerous structural and functional analyses. Also demonstrates that the motor domain includes the globular head structure seen in earlier electron microscopy images.**

82. Nishiura, M. *et al.* A single-headed recombinant fragment of *Dictyostelium* cytoplasmic dynein can drive the robust sliding of microtubules. *J. Biol. Chem.* **279**, 22799–22802 (2004).

83. Reck-Peterson, S. L. *et al.* Single-molecule analysis of dynein processivity and stepping behavior. *Cell* **126**, 335–348 (2006).
    **Establishes *S. cerevisiae* as another important cytoplasmic dynein expression system and provides insight into the requirements for processive dynein motion.**

84. Höök, P. *et al.* Long range allosteric control of cytoplasmic dynein ATPase activity by the stalk and C-terminal domains. *J. Biol. Chem.* **280**, 33045–33054 (2005).

85. Imamula, K., Kon, T., Ohkura, R. & Sutoh, K. The coordination of cyclic microtubule association/dissociation and tail swing of cytoplasmic dynein. *Proc. Natl Acad. Sci. USA* **104**, 16134–16139 (2007).

86. Mogami, T., Kon, T., Ito, K. & Sutoh, K. Kinetic characterization of tail swing steps in the ATPase cycle of *Dictyostelium* cytoplasmic dynein. *J. Biol. Chem.* **282**, 21639–21644 (2007).

87. Johnson, K. A. Pathway of the microtubule–dynein ATPase and the structure of dynein: a comparison with actomyosin. *Annu. Rev. Biophys. Biophys. Chem.* **14**, 161–188 (1985).

88. Samsó, M., Radermacher, M., Frank, J. & Koonce, M. P. Structural characterization of a dynein motor domain. *J. Mol. Biol.* **276**, 927–937 (1998).

89. Gee, M. A., Heuser, J. E. & Vallee, R. B. An extended microtubule-binding structure within the dynein motor domain. *Nature* **390**, 636–639 (1997).

90. Roberts, A. J. *et al.* ATP-driven remodeling of the linker domain in the dynein motor. *Structure* **20**, 1670–1680 (2012).
    **A 2D and 3D electron microscopy study of an axonemal and cytoplasmic dynein, revealing that the linker domain is a stable structural entity that is remodelled by the AAA+ ring.**

91. Roberts, A. *et al.* AAA+ ring and linker swing mechanism in the dynein motor. *Cell* **136**, 485–495 (2009).

92. Burgess, S. A., Walker, M. L., Sakakibara, H., Knight, P. J. & Oiwa, K. Dynein structure and power stroke. *Nature* **421**, 715–718 (2003).

93. Kon, T. *et al.* The 2.8Å crystal structure of the dynein motor domain. *Nature* **484**, 345–350 (2012).
**Reports a high-resolution crystal structure of the *D. discoideum* dynein motor domain in the ADP-bound state. Structure-guided mutagenesis provides insight into how the linker domain moves and the roles of the AAA + modules, strut and C-terminal sequence in allosteric communication.**
94. Kon, T., Sutoh, K. & Kurisu, G. X-ray structure of a functional full-length dynein motor domain. *Nature Struct. Mol. Biol.* **18**, 638–642 (2011).
95. Schmidt, H., Gleave, E. S. & Carter, A. P. Insights into dynein motor domain function from a 3.3-Å crystal structure. *Nature Struct. Mol. Biol.* **19**, 492–497 (2012).
**Reports a high-resolution structure of the *S. cerevisiae* dynein motor domain, crystallized in the absence of nucleotide. Crystal-soaking experiments reveal distinct nucleotide-binding behaviours in AAA1–AAA4, and mutagenesis suggests a functional role for linker docking at AAA5.**
96. Carter, A. P., Cho, C., Jin, L. & Vale, R. D. Crystal structure of the dynein motor domain. *Science* **331**, 1159–1165 (2011).
97. Glynn, S. E., Martin, A., Nager, A. R., Baker, T. A. & Sauer, R. T. Structures of asymmetric ClpX hexamers reveal nucleotide-dependent motions in a AAA + protein-unfolding machine. *Cell* **139**, 744–756 (2009).
98. Wang, J. *et al.* Nucleotide-dependent conformational changes in a protease-associated ATPase HsIU. *Structure* **9**, 1107–1116 (2001).
99. Gibbons, I. R. *et al.* Photosensitized cleavage of dynein heavy chains. Cleavage at the "V1 site" by irradiation at 365 nm in the presence of ATP and vanadate. *J. Biol. Chem.* **262**, 2780–2786 (1987).
100. Kon, T., Nishiura, M., Ohkura, R., Toyoshima, Y. Y. & Sutoh, K. Distinct functions of nucleotide-binding/hydrolysis sites in the four AAA modules of cytoplasmic dynein. *Biochemistry* **43**, 11266–11274 (2004).
101. Enemark, E. J. & Joshua-Tor, L. Mechanism of DNA translocation in a replicative hexameric helicase. *Nature* **442**, 270–275 (2006).
102. Cho, C., Reck-Peterson, S. & Vale, R. Cytoplasmic dynein's regulatory ATPase sites affect processivity and force generation. *J. Biol. Chem.* **283**, 25839–25845 (2008).
103. Huang, J., Roberts, A. J., Leschziner, A. E. & Reck-Peterson, S. L. Lis1 acts as a "clutch" between the ATPase and microtubule-binding domains of the dynein motor. *Cell* **150**, 975–986 (2012).
104. McKenney, R. J., Vershinin, M., Kunwar, A., Vallee, R. B. & Gross, S. P. LIS1 and NudE induce a persistent dynein force-producing state. *Cell* **141**, 304–314 (2010).
105. Yamada, M. *et al.* LIS1 and NDEL1 coordinate the plus-end-directed transport of cytoplasmic dynein. *EMBO J.* **27**, 2471–2483 (2008).
106. Cho, C. & Vale, R. D. The mechanism of dynein motility: insight from crystal structures of the motor domain. *Biochim. Biophys. Acta* **1823**, 182–191 (2011).
107. Numata, N., Shima, T., Ohkura, R., Kon, T. & Sutoh, K. C-Sequence of the *Dictyostelium* cytoplasmic dynein participates in processivity modulation. *FEBS Lett.* **585**, 1185–1190 (2011).
108. Hwang, W. & Lang, M. J. Nucleotide-dependent control of internal strains in ring-shaped AAA + motors. *Cell. Mol. Bioeng.* **6**, 65–73 (2013).
109. Gibbons, I. R. *et al.* The affinity of the dynein microtubule-binding domain is modulated by the conformation of its coiled-coil stalk. *J. Biol. Chem.* **280**, 23960–23965 (2005).
110. Carter, A. P. *et al.* Structure and functional role of dynein's microtubule-binding domain. *Science* **322**, 1691–1695 (2008).
111. Kon, T. *et al.* Helix sliding in the stalk coiled coil of dynein couples ATPase and microtubule binding. *Nature Struct. Mol. Biol.* **16**, 325–333 (2009).
112. Redwine, W. B. *et al.* Structural basis for microtubule binding and release by dynein. *Science* **337**, 1532–1536 (2012).
**References 109–112 provide evidence for the helix-sliding hypothesis for allosteric communication through the stalk of dynein, which was put forward in reference 109. Reference 112 also provides insight into the structural changes within the microtubule-binding domain of dynein.**
113. Sweeney, H. L. & Houdusse, A. The motor mechanism of myosin V: insights for muscle contraction. *Philo. Trans. R. Soc. Lond. B* **359**, 1829–1841 (2004).
114. Xi, Z., Gao, Y., Sirinakis, G., Guo, H. & Zhang, Y. Single-molecule observation of helix staggering, sliding, and coiled coil misfolding. *Proc. Natl Acad. Sci. USA* **109**, 5711–5716 (2012).
115. Burgess, S. A., Walker, M. L., Sakakibara, H., Oiwa, K. & Knight, P. J. The structure of dynein-c by negative stain electron microscopy. *J. Struct. Biol.* **146**, 205–216 (2004).
116. Burgess, S. A. & Knight, P. J. Is the dynein motor a winch? *Curr. Opin. Struct. Biol.* **14**, 138–146 (2004).
117. Gennerich, A., Carter, A. P., Reck-Peterson, S. L. & Vale, R. D. Force-induced bidirectional stepping of cytoplasmic dynein. *Cell* **131**, 952–965 (2007).
118. Kon, T., Mogami, T., Ohkura, R., Nishiura, M. & Sutoh, K. ATP hydrolysis cycle-dependent tail motions in cytoplasmic dynein. *Nature Struct. Mol. Biol.* **12**, 513–519 (2005).
119. Shima, T., Kon, T., Imamula, K., Ohkura, R. & Sutoh, K. Two modes of microtubule sliding driven by cytoplasmic dynein. *Proc. Natl Acad. Sci. USA* **103**, 17736–17740 (2006).
120. Ueno, H., Yasunaga, T., Shingyoji, C. & Hirose, K. Dynein pulls microtubules without rotating its stalk. *Proc. Natl Acad. Sci. USA* **105**, 19702–19707 (2008).
121. Movassagh, T., Bui, K. H., Sakakibara, H., Oiwa, K. & Ishikawa, T. Nucleotide-induced global conformational changes of flagellar dynein arms revealed by *in situ* analysis. *Nature Struct. Mol. Biol.* **17**, 761–767 (2010).
122. Qiu, W. *et al.* Dynein achieves processive motion using both stochastic and coordinated stepping. *Nature Struct. Mol. Biol.* **19**, 193–200 (2012).
123. Dewitt, M. A., Chang, A. Y., Combs, P. A. & Yildiz, A. Cytoplasmic dynein moves through uncoordinated stepping of the AAA + ring domains. *Science* **335**, 221–225 (2011).
**References 122 and 123 use two-colour single-molecule experiments to reveal that *S. cerevisiae* cytoplasmic dynein dimers can move processively along the microtubule without following a strict stepping pattern. Analysis of the stepping traces provides insight into the spatial configuration of the motor domains and their loose, tension-based coordination.**
124. Veigel, C., Wang, F., Bartoo, M. L., Sellers, J. R. & Molloy, J. E. The gated gait of the processive molecular motor, myosin V. *Nature Cell Biol.* **4**, 59–65 (2002).
125. Shima, T., Imamula, K., Kon, T., Ohkura, R. & Sutoh, K. Head-head coordination is required for the processive motion of cytoplasmic dynein, an AAA + molecular motor. *J. Struct. Biol.* **156**, 182–189 (2006).
126. Stinson, B. M. *et al.* Nucleotide binding and conformational switching in the hexameric ring of a AAA + machine. *Cell* **153**, 628–639 (2013).
127. Sakamoto, T., Webb, M. R., Forgacs, E., White, H. D. & Sellers, J. R. Direct observation of the mechanochemical coupling in myosin Va during processive movement. *Nature* **455**, 128–132 (2008).
128. Firestone, A. J. *et al.* Small-molecule inhibitors of the AAA + ATPase motor cytoplasmic dynein. *Nature* **484**, 125–129 (2012).
129. Kamiya, R. Functional diversity of axonemal dyneins as studied in *Chlamydomonas* mutants. *Int. Rev. Cytol.* **219**, 115–155 (2002).
130. Kikushima, K. & Kamiya, R. Clockwise translocation of microtubules by flagellar inner-arm dyneins *in vitro*. *Biophys. J.* **94**, 4014–4019 (2008).
131. Mallik, R., Carter, B. C., Lex, S. A., King, S. J. & Gross, S. P. Cytoplasmic dynein functions as a gear in response to load. *Nature* **427**, 649–652 (2004).
132. Rai, A. K., Rai, A., Ramaiya, A. J., Jha, R. & Mallik, R. Molecular adaptations allow dynein to generate large collective forces inside cells. *Cell* **152**, 172–182 (2013).
133. Schroeder, H. W., Mitchell, C., Shuman, H., Holzbaur, E. L. F. & Goldman, Y. E. Motor number controls cargo switching at actin-microtubule intersections *in vitro*. *Curr. Biol.* **20**, 687–696 (2010).
134. Toba, S., Watanabe, T. M., Yamaguchi-Okimoto, L., Toyoshima, Y. Y. & Higuchi, H. Overlapping hand-over-hand mechanism of single molecular motility of cytoplasmic dynein. *Proc. Natl Acad. Sci. USA* **103**, 5741–5745 (2006).
135. Walter, W. J., Koonce, M. P., Brenner, B. & Steffen, W. Two independent switches regulate cytoplasmic dynein's processivity and directionality. *Proc. Natl Acad. Sci. USA* **109**, 5289–5293 (2012).
136. Ross, J. L., Wallace, K., Shuman, H., Goldman, Y. E. & Holzbaur, E. L. F. Processive bidirectional motion of dynein-dynactin complexes *in vitro*. *Nature Cell Biol.* **8**, 562–570 (2006).
137. Ananthanarayanan, V. *et al.* Dynein motion switches from diffusive to directed upon cortical anchoring. *Cell* **153**, 1526–1536 (2013).
138. Nicastro, D. *et al.* Cryo-electron tomography reveals conserved features of doublet microtubules in flagella. *Proc. Natl Acad. Sci. USA* **108**, E845–E853 (2011).
139. Summers, K. E. & Gibbons, I. R. Adenosine triphosphate-induced sliding of tubules in trypsin-treated flagella of sea-urchin sperm. *Proc. Natl Acad. Sci.* **68**, 3092–3096 (1971).
140. Nicastro, D. Cryo-electron microscope tomography to study axonemal organization. *Methods Cell Biol.* **91**, 1–39 (2009).
141. Hom, E. F. *et al.* A unified taxonomy for ciliary dyneins. *Cytoskeleton (Hoboken)* **68**, 555–565 (2011).
142. Bui, K. H., Yagi, T., Yamamoto, R., Kamiya, R. & Ishikawa, T. Polarity and asymmetry in the arrangement of dynein and related structures in the *Chlamydomonas axoneme*. *J. Cell Biol.* **198**, 913–925 (2012).
143. Kagami, O. & Kamiya, R. Translocation and rotation of microtubules caused by multiple species of *Chlamydomonas* inner-arm dynein. *J. Cell Sci.* **103**, 653–664 (1992).
144. Yagi, T., Uematsu, K., Liu, Z. & Kamiya, R. Identification of dyneins that localize exclusively to the proximal portion of *Chlamydomonas* flagella. *J. Cell Sci.* **122**, 1306–1314 (2009).
145. Woolley, D. M. Studies on the eel sperm flagellum. I. The structure of the inner dynein arm complex. *J. Cell Sci.* **110**, 85–94 (1997).
146. Zhang, X. & Wigley, D. The 'glutamate switch' provides a link between ATPase activity and ligand binding in AAA + proteins. *Nature Struct. Mol. Biol.* **15**, 1223–1227 (2008).
147. Hanson, P. I. & Whiteheart, S. W. AAA + proteins: have engine, will work. *Nature Rev. Mol. Cell Biol.* **6**, 519–529 (2005).
148. Pfister, K. K. *et al.* Cytoplasmic dynein nomenclature. *J. Cell Biol.* **171**, 411–413 (2005).
149. Mizuno, N. *et al.* Dynein and kinesin share an overlapping microtubule-binding site. *EMBO J.* **23**, 2459–2467 (2004).

**SUPPLEMENTARY INFORMATION**
See online article: S1 (table)

**ALL LINKS ARE ACTIVE IN THE ONLINE PDF**